




# Competitive Growth Enhances Conditional Growth Mutant Sensitivity to Antibiotics and Exposes a Two-Component System as an Emerging Antibacterial Target in *Burkholderia cenocepacia*

April S. Gislason,<sup>a</sup> Matthew Choy,<sup>a</sup> Ruhi A. M. Bloodworth,<sup>a</sup> Wubin Qu,<sup>b</sup> Maria S. Stietz,<sup>a</sup> Xuan Li,<sup>c</sup> Chenggang Zhang,<sup>b</sup>  Silvia T. Cardona<sup>a,d</sup>

Department of Microbiology, University of Manitoba, Winnipeg, Manitoba, Canada<sup>a</sup>; Beijing Institute of Radiation Medicine, State Key Laboratory of Proteomics, Cognitive and Mental Health Research Center, Beijing, China<sup>b</sup>; Department of Mathematics and Statistics, University of Minnesota Duluth, Duluth, Minnesota, USA<sup>c</sup>; Department of Medical Microbiology and Infectious Disease, University of Manitoba, Winnipeg, Canada<sup>d</sup>

**ABSTRACT** Chemogenetic approaches to profile an antibiotic mode of action are based on detecting differential sensitivities of engineered bacterial strains in which the antibacterial target (usually encoded by an essential gene) or an associated process is regulated. We previously developed an essential-gene knockdown mutant library in the multidrug-resistant *Burkholderia cenocepacia* by transposon delivery of a rhamnose-inducible promoter. In this work, we used Illumina sequencing of multiplex-PCR-amplified transposon junctions to track individual mutants during pooled growth in the presence of antibiotics. We found that competition from nontarget mutants magnified the hypersensitivity of a clone underexpressing *gyrB* to novobiocin by 8-fold compared with hypersensitivity measured during clonal growth. Additional profiling of various antibiotics against a pilot library representing most categories of essential genes revealed a two-component system with unknown function, which, upon depletion of the response regulator, sensitized *B. cenocepacia* to novobiocin, ciprofloxacin, tetracycline, chloramphenicol, kanamycin, meropenem, and carbonyl cyanide 3-chlorophenylhydrazone, but not to colistin, hydrogen peroxide, and dimethyl sulfoxide. We named the gene cluster *esaSR* for enhanced sensitivity to antibiotics sensor and response regulator. Mutational analysis and efflux activity assays revealed that while *esaS* is not essential and is involved in antibiotic-induced efflux, *esaR* is an essential gene and regulates efflux independently of antibiotic-mediated induction. Furthermore, microscopic analysis of cells stained with propidium iodide provided evidence that depletion of *EsaR* has a profound effect on the integrity of cell membranes. In summary, we unraveled a previously uncharacterized two-component system that can be targeted to reduce antibiotic resistance in *B. cenocepacia*.

**KEYWORDS** *Burkholderia*, Illumina, antibiotic profiling, antibiotic resistance, drug efflux, drug targets, essential genes, Gram-negative bacteria, transposon mutant, two-component regulatory systems

The increasing occurrence of infections by multidrug-resistant bacteria has become a global concern (1). Moreover, there is a high demand to develop new therapeutics against multidrug-resistant Gram-negative bacteria, as they are predicted to be the biggest threats (2). One example is *Burkholderia cenocepacia*, which belongs to the

Received 13 April 2016 Returned for modification 17 August 2016 Accepted 26 October 2016

Accepted manuscript posted online 31 October 2016

**Citation** Gislason AS, Choy M, Bloodworth RAM, Qu W, Stietz MS, Li X, Zhang C, Cardona ST. 2017. Competitive growth enhances conditional growth mutant sensitivity to antibiotics and exposes a two-component system as an emerging antibacterial target in *Burkholderia cenocepacia*. *Antimicrob Agents Chemother* 61:e00790-16. <https://doi.org/10.1128/AAC.00790-16>.

**Copyright** © 2016 American Society for Microbiology. All Rights Reserved. Address correspondence to Silvia T. Cardona, [Silvia.Cardona@umanitoba.ca](mailto:Silvia.Cardona@umanitoba.ca).

**TABLE 1** Bacterial strains and plasmids

Strain or plasmid	Features <sup>a</sup>	Source
<i>B. cenocepacia</i> K56-2	Cystic fibrosis clinical isolate	82
<i>B. cenocepacia</i> MKC2	Site-directed CG mutant; <i>PrhaB</i> promoter replacement of <i>esaR</i>	This study
<i>B. cenocepacia</i> MKC4	<i>DesaS</i>	This study
<i>E. coli</i> SY327	<i>araD</i> $\Delta$ ( <i>lac pro</i> ) <i>argE</i> (Am) <i>recA56</i> Rif <sup>r</sup> <i>nalA</i> $\lambda$ <i>pir</i>	83
Plasmids		
pRK2013	<i>ori</i> <sub>colE1</sub> ; RK2 derivative; Kan <sup>+</sup> <i>mob</i> <sup>+</sup> <i>tra</i> <sup>+</sup>	84
pSC201	<i>ori</i> <sub>R6K</sub> ; <i>rhaR rhaS Prha B dhfr</i>	30
pMC2	pSC201 derivative; <i>ori</i> <sub>R6K</sub> ; <i>rhaR rhaS PrhaB dhfr</i>	This study
pGPI-Scel	<i>ori</i> <sub>R6K</sub> ; Tmp <sup>r</sup> ; <i>mob</i> <sup>+</sup> ; carries I-Scel cut site	31
pMC4	pGPI-Scel containing upstream and downstream regions of <i>esaS</i>	This study
pMC5	pGPI-Scel containing upstream and downstream regions of <i>esaSR</i>	This study
pDAI-Scel	<i>ori</i> <sub>PBBR1</sub> ; Tet <sup>r</sup> ; <i>mob</i> <sup>+</sup> ; <i>P</i> <sub><i>dhfr</i></sub> ; I-Scel gene	31

<sup>a</sup>Kan, kanamycin; Tmp, trimethoprim; Tet, tetracycline; *tra*<sup>+</sup>, self transferable; *mob*<sup>+</sup>, mobilizable.

*Burkholderia cepacia* complex (Bcc), opportunistic pathogens that cause lung infections in immunocompromised and cystic fibrosis (CF) patients (3). *B. cenocepacia* is inherently multidrug resistant, owing to an impermeable outer membrane (4) and diverse metabolic (5) and efflux (6) capabilities, and is capable of developing additional resistance to all classes of antibiotics *in vivo*, prohibiting effective antibiotic treatment (7). Despite the severity of Bcc infections and the high antibiotic resistance of Bcc isolates, there are very few efforts to develop alternative drugs for treatment. Furthermore, there is very little understanding of how antibiotic resistance is regulated and can be targeted to increase the usefulness of current antibiotics to treat Bcc infections.

Identifying novel antibacterial targets and targets for antibiotic adjuvant therapy is an important step in the antibacterial drug discovery pipeline (8, 9). Chemogenetic approaches (10, 11), where underexpression of single essential gene product sensitizes strains to specific inhibitors of the products, are useful to identify targets and processes affected by small molecules with unknown mechanisms of action (MOA) (12, 13). Generating mutant profiles for antibiotics becomes more informative as the diversity of the mutant library increases. To modulate essential gene expression, antisense RNA induction (14, 15) and systematic replacement of essential gene promoters with inducible systems (16–19) have been employed. Recently, CRISPR interference (20) was used to generate the first bacterial comprehensive essential gene knockdown library (21). However, these methodologies are not without challenges, as they employ bacterial mutants grown clonally. Bacterial growth is measured by optical density (in liquid medium) or colony size (on solid medium). Hundreds of microtiter plates, robotic equipment, and specific standardization methods are required to minimize the systematic variation and batch effects across plates (22). Using an Illumina next-generation-sequencing platform (23), a method to profile a library of loss-of-function *Saccharomyces cerevisiae* strains in response to small molecules was developed (25). This is in contrast to approaches to determine the targets of antibiotics (24), which have not yet taken advantage of the sensitivity, dynamic range (25), and throughput of detection by next-generation sequencing.

We previously developed a library of 106 *B. cenocepacia* K56-2 conditional growth (CG) mutants (Table 1) (26) expressing suboptimal levels of essential genes from a rhamnose-inducible promoter (27). Here, we developed a method for tracking the relative abundances of pooled conditional growth mutants after exposure to several antibiotics by Illumina sequencing of the transposon insertion tags after amplification by multiplex PCR. Although our method limited the number of mutants that could be included in the assay, antibiotic profiling revealed a CG mutant of an uncharacterized two-component signal transduction system (TCS) that was hypersensitive to several antibiotics. Genetic analysis, efflux activity assays, and microscopy provided further

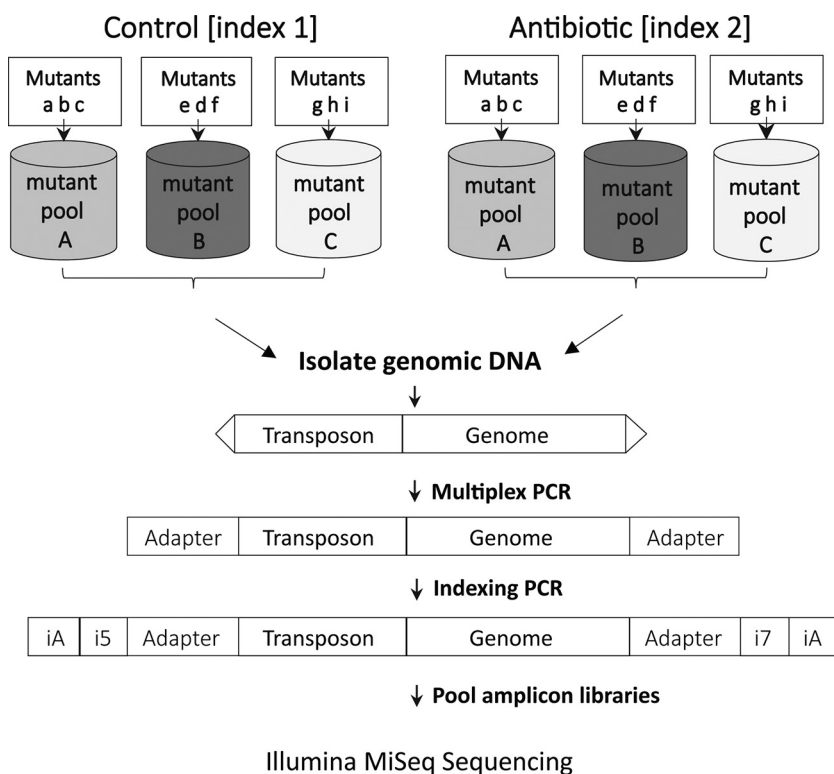


**FIG 1** Detection of CG mutant enhanced sensitivity using Illumina MiSeq. Mutants with similar rhamnose sensitivities (mutants a, b, and c; e, d, and f; and g, h, and i) were pooled in equal amounts (pools A, B, and C) and incubated with and without antibiotic. The CG mutant pools were combined, genomic DNA was extracted, and the transposon-genome interface was amplified by multiplex PCR using a common transposon-specific forward primer and a genome-specific reverse primer, both of which contained 5' adapter sequences (Adapter). The index PCR added indexes to the amplicons using primers complementary to the adapter sequences and containing 5' indexes (i5 and i7) and Illumina MiSeq-specific adapter sequences (iA). The amplicons were then sequenced in one run of a MiSeq, and the reads, separated by treatment, containing transposon insertion sites were assigned to their corresponding CG mutants. The RAs of reads corresponding to each CG mutant within the total reads per index were calculated, and CG mutant depletion in response to an antibiotic was expressed as the ratio between the control RA and the antibiotic RA.

evidence that the TCS is involved in controlling multidrug efflux and cell membrane integrity, exposing a novel target for antibiotic drug therapy in the Bcc.

## RESULTS

**Quantification of CG mutant relative abundance by Illumina sequencing of multiplex-PCR-amplified transposon junctions.** Our original CG mutant library consisted of 106 mutants in which the rhamnose-inducible promoter controls the expression of essential genes in 50 unique operons (26). Taking advantage of this transposon mutant library, we developed a method to detect the enhanced sensitivity of CG mutants when they are grown competitively in the presence of an antibiotic (Fig. 1). The strategy involved pooled growth experiments in which CG mutants with similar rhamnose dose-response curves (see Fig. S1 in the supplemental material) were exposed to several antibiotics. CG mutant pools that received the same treatment were combined, the genomic DNA was extracted, and the transposon-genome interface was amplified by multiplex PCR. The amplicons were then Illumina sequenced, and the relative abundance (RA) of each CG mutant was calculated for each treatment.

In order to avoid possible misidentification of CG mutants due to the presence of close transposon insertions, we selected 56 CG mutants from the original CG mutant library (26) that had insertion sites located at least 10 kb from each other in the genome. To determine the amplification reproducibility of the transposon-genome junctions of the individual CG mutants, the pooled genomic DNA of equal amounts of

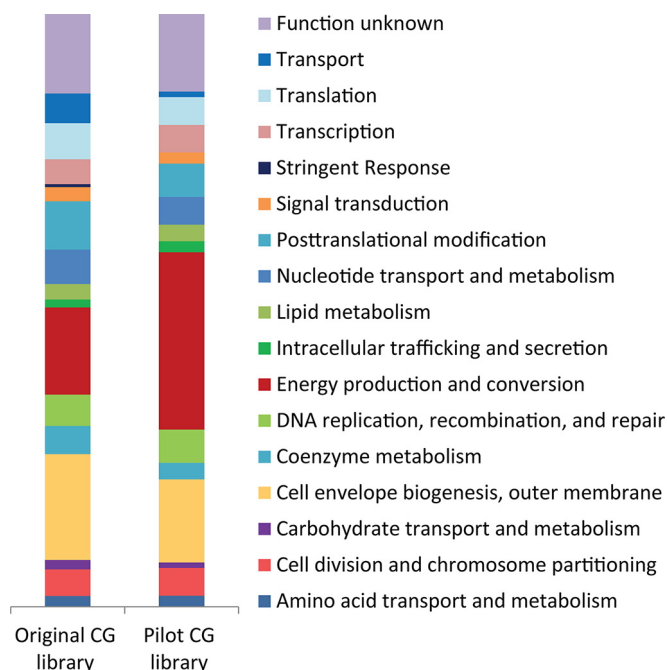


**FIG 2** Functional categories represented by CG mutants in the original (106 mutants) and pilot (25 mutants) CG libraries. Sixteen out of the 17 functional categories, determined by the GO (Gene Ontology) and COG (Cluster of Orthologous Genes) annotations, identified in the original mutant library (26) are represented in the pilot CG library. The proportion of each category is based on the functions of annotated genes in the *B. cenocepacia* J2315 genome that are predicted to be in an operon downstream of the transposon insertion site.

CG mutants was extracted and used as the template in the multiplex PCR, and the resulting amplicons were sequenced on an Illumina MiSeq. Initially, 2 CG mutant amplicons (67-10H9 and 86-3D16) accounted for 30% of the total reads, 12 had read counts that varied between replicates, and 19 were not detected. To increase the sequencing depth and improve the amplification of the variably amplified and undetected amplicons, the primer concentrations for 67-10H9 and 86-3D16 were decreased to reduce the overrepresented amplicons (see Table S2 in the supplemental material). Adjusting the primer concentrations increased the sequencing depth of the other amplicons in the library (data not shown) while maintaining the reproducible detection of 25 CG mutants (see Fig. S2 in the supplemental material). However, detection and reproducibility were not improved for the variably amplified and undetected CG mutants. A pilot CG library comprised of the 25 CG mutants that had reproducible amplification in the multiplex PCR was then used to profile antibiotics. Despite its small size, the pilot CG library contains representatives of 25 unique essential operons covering the main essential functional categories identified in the original CG mutant library (26) (Fig. 2).

To demonstrate that we could detect CG mutant depletion by multiplexed Illumina sequencing, the ratios of the CG mutants were artificially adjusted to mimic antibiotic-driven mutant depletion. Five CG mutant pools were generated: pool A contained all the mutants in the pilot CG library combined in equal amounts (based on the optical density at 600 nm [ $OD_{600}$ ]), and pools B to D contained the majority of mutants pooled in equal amounts, with 2 to 8 CG mutants in each pool depleted by 10-fold or 100-fold with respect to pool A. The observed depletion of CG mutants was representative of the initial concentrations (10-fold or 100-fold) of each mutant within the pools. The percent abundance of each CG mutant in the pools from duplicate multiplex PCRs was consistent, showing that each CG mutant was reproducibly amplified and detected (see Fig. S3 in the supplemental material). Therefore, sequencing amplicons from the multiplex PCR accurately measured CG mutant depletion in the pilot CG library.

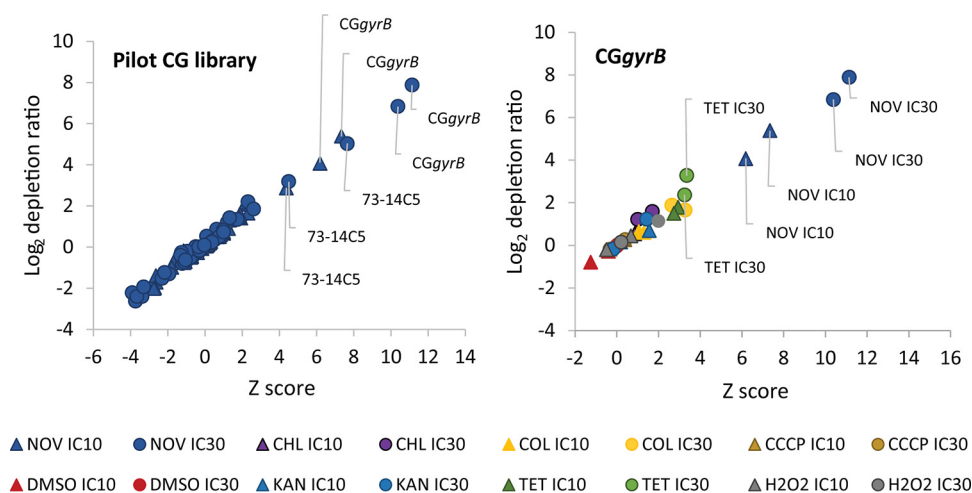


**FIG 3** Competitive ESA detects the sensitization of *CGgyrB* to novobiocin.  $\log_2$  depletion ratios and Z scores from two independent experiments are overlaid. (Left) CG mutant enhanced sensitivity to novobiocin. CG mutants showing enhanced sensitivity to novobiocin are labeled. (Right) Antibiotic profile of the GyrB-depleted *CGgyrB* mutant. Antibiotics causing enhanced sensitivity are labeled.

**A competitive enhanced-sensitivity assay enhanced the specific depletion of the *CGgyrB* mutant to its cognate antibiotic, novobiocin.**

To sensitize CG mutants to antibiotics, we used rhamnose concentrations that allowed 30 to 60% of wild-type (WT) growth, as previously determined (26). Pools of mutants with similar responses to rhamnose were made and grown in the presence or absence of antibiotics. Cultures exposed to the same treatment were combined by volume, and the genomic DNA was extracted and used as a template in a two-step PCR in which a unique index identified the treatment. The CG mutant 58-14E1, referred to here as *CGgyrB*, was included in the pilot CG library. This mutant strain was sensitized to produce suboptimal levels of the DNA gyrase subunit GyrB, which is the target of novobiocin (NOV) (28). A bioactive target match was evident in the competitive enhanced-sensitivity assay (ESA), in which exposure to sublethal concentrations of novobiocin caused more than 10-fold depletion of the sensitized *CGgyrB* (Fig. 3). *CGgyrB* also showed enhanced sensitivity to the tetracycline (TET) 10% ( $IC_{10}$ ) and 30% ( $IC_{30}$ ) inhibitory concentrations (the concentrations of antibiotic inhibiting 10% or 30% of wild-type growth, respectively), with  $\log_2$  depletion ratios at or slightly above the cutoff level of significance, respectively, and Z scores higher than 2 for both conditions (Fig. 3, right). The  $\log_2$  depletion ratio of *CGgyrB* in response to the colistin (COL)  $IC_{30}$  was slightly below 2, while the Z score was above the cutoff level of significance. However, *CGgyrB* was not hypersensitive to the colistin  $IC_{10}$ , as the  $\log_2$  depletion ratio and Z score were lower than 2. Similarly, *CGgyrB* did not show enhanced sensitivity to the other antibiotics tested (Fig. 3, right), and with the exception of mutant 73-14C5 (see below), the CG mutants were not sensitive to novobiocin (Fig. 3, left). Altogether, the assay was able to detect specific sensitivity of *CGgyrB* to its corresponding antibiotic.

Estimating bacterial growth by turbidimetry or colony size is limited by the detection range of the spectrophotometer or the resolution of the visualization tool used, respectively. Tracking bacterial growth by Illumina sequencing should have a greater detection range limited only by the depth of coverage. In addition, Illumina sequencing allows mutant detection during competitive growth. To investigate the contribution of competitive growth to the specific enhanced sensitivity of *CGgyrB* when exposed to novobiocin, *CGgyrB* was grown in a pool at one rhamnose concentration with 3 other CG mutants, and their relative abundances were compared when they were grown competitively in a pool or grown clonally by Illumina sequencing. The depletion of *CGgyrB* in response to novobiocin was greater than 17-fold when grown in coculture with 3 other CG mutants and 2-fold when grown clonally (Table 2). Competitive growth

**TABLE 2** Comparison of enhanced sensitivities of pooled and clonally grown CG mutants

Growth; measurement <sup>a</sup>	Fold depletion <sup>b</sup>			
	CGgyrB	67-5H10	86-3D16	96-1K12
NOV pool; NGS	17.16 (2.81)	1.36 (0.39)	1.09 (0.13)	0.64 (0.20)
NOV clonal; NGS	2.37 (0.30)	1.11 (0.20)	1.13 (0.08)	0.80 (0.05)
NOV clonal; OD <sub>600</sub>	2.60 (0.09)	1.19 (0.05)	1.13 (0.12)	0.87 (0.06)
CHL pool; NGS	1.17 (0.11)	1.03 (0.23)	0.75 (0.12)	0.92 (0.04)
CHL clonal; NGS	0.88 (0.05)	1.09 (0.18)	1.16 (0.16)	1.03 (0.04)
CHL clonal; OD <sub>600</sub>	1.16 (0.12)	1.45 (0.03)	1.30 (0.10)	1.22 (0.04)
No ATB pool/no ATB clonal; NGS	1.07 (0.35)	0.99 (0.38)	1.27 (0.07)	0.93 (0.01)

<sup>a</sup>ATB, antibiotic; NGS, next-generation sequencing.

<sup>b</sup>Means (standard deviations) of the results of two independent experiments.

did increase the sensitization of CGgyrB when exposed to an IC<sub>10</sub> of novobiocin, but not an IC<sub>10</sub> of chloramphenicol (CHL). The fold depletion of clonally grown strains measured by Illumina sequencing was consistent with that calculated by measuring the OD<sub>600</sub> (Table 2). The observed low sensitivity of the clonal enhanced-sensitivity assay was expected, as novobiocin was used at the very low IC<sub>10</sub>. However, this slight inhibitory concentration was sufficient to cause severe depletion of the CGgyrB mutant growing within the pool. These results demonstrate that competitive growth can enhance the specific sensitivity of a CG mutant to its cognate antibiotic.

**The competitive enhanced-sensitivity assay revealed a TCS involved in regulation of antibiotic resistance.** The transposon insertion of mutant 73-14C5 is located 58 bp upstream of the 3' end of the BURCENK56V\_RS04770 locus, which seems to form an operon with the downstream gene BURCENK56V\_RS04765. While it is not clear whether the transposon insertion in mutant 73-14C5 functionally disrupted RS04770, RS04765 is under the control of the rhamnose promoter. In the *B. cenocepacia* K56-2 draft genome (29), RS04770 and RS04765 are preliminarily annotated as a histidine kinase-coding gene and an XRE family transcriptional regulator gene, respectively, suggesting that they form a TCS. These genes are homologs of BCAL0471 and BCAL0472, respectively, in the complete *B. cenocepacia* J2315 genome (3). By profiling the pilot CG library with several growth inhibitors, we found that the CG mutant 73-14C5 had significant depletion ratios in response to novobiocin (Fig. 3A and 4A), chloramphenicol, tetracycline, kanamycin (KAN), and carbonyl cyanide *m*-chlorophenylhydrazine (CCCP) (Fig. 4A). CG mutant 73-14C5 was not sensitive to hydrogen peroxide (H<sub>2</sub>O<sub>2</sub>), colistin, or dimethyl sulfoxide (DMSO). The enhanced sensitivity of 73-14C5 to antibiotics tested in the competitive ESA, as well as ciprofloxacin (CIP) and meropenem (MER), was confirmed by growing the strains clonally and calculating the depletion ratio based on the OD<sub>600</sub>s of the cultures. In agreement with the results from the competitive ESA, mutant 73-14C5 showed a similar antibiotic profile and also demonstrated enhanced sensitivity to ciprofloxacin and meropenem (Fig. 4B). The CG mutants 79-30H5 and 81-36C9 (26), which contain the transposon insertion in the same location and were independently obtained, showed similar profiles (data not shown). Taken together, these results show that this TCS is involved in resistance to different classes of antibiotics, including inhibitors of cell wall synthesis (meropenem), DNA replication (novobiocin and ciprofloxacin), and protein synthesis (tetracycline, kanamycin, and chloramphenicol). The RS04770 and RS04765 genes were designated *esaS* and *esaR*, respectively.

**Mutational analysis of the *esaSR* locus suggests that *esaR* is an essential gene.**

The transposon insertion site within the 3' end of *esaS* and upstream of *esaR* in 73-14C5 suggested that the CG phenotype was due to downregulation of *esaR* in the absence of rhamnose. In the majority of our CG mutant library, downregulation of essential genes by the rhamnose-inducible promoter resulted in the absence of growth (26). Instead, 73-14C5 displayed 50% of wild-type growth in the absence of rhamnose (Fig. 5A), suggesting that downregulation of *esaR* expression caused a fitness defect but that the gene was not essential. Alternatively, low protein turnover or leaky levels of

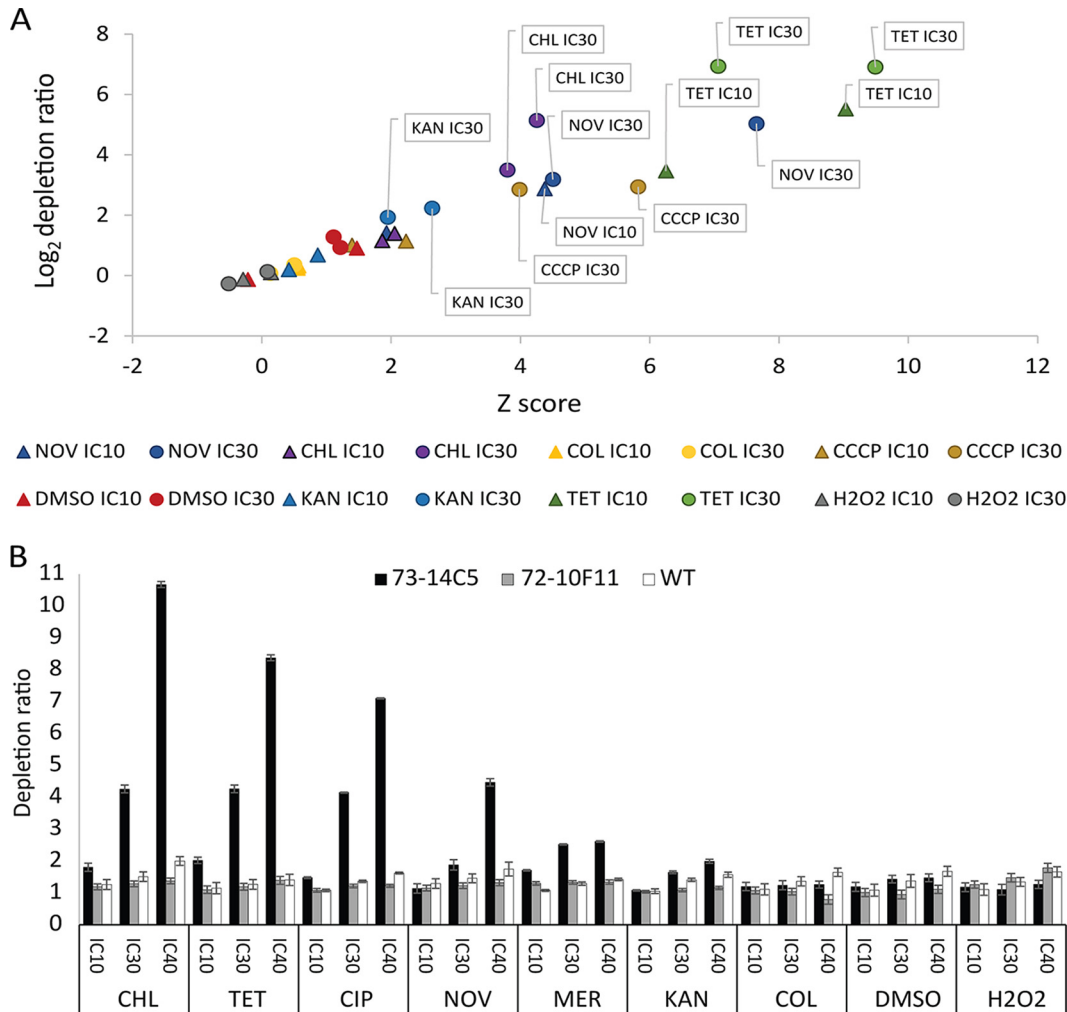


**FIG 4** Antibiotic profile of CG mutant 73-14C5, underexpressing EsaR. (A) Antibiotic profile of CG mutant 73-14C5 from the competitive ESA. Log<sub>2</sub> depletion ratios and Z scores for each antibiotic treatment from two independent experiments are overlaid. Antibiotics causing hypersensitivity are labeled. (B) Enhanced sensitivity measured by OD<sub>600</sub>. Shown are the depletion ratios of 73-14C5, 72-10F11 (the CG mutant cocultured with 73-14C5 in the competitive ESA), and *B. cenocepacia* K56-2 WT strain in response to antibiotics. The depletion ratio was calculated by dividing the OD<sub>600</sub> of the no-antibiotic control by the OD<sub>600</sub> under the antibiotic condition. The error bars represent the standard deviations of the results of three independent experiments.

expression from the rhamnose-inducible promoter even in the absence of rhamnose may provide cellular levels of an essential protein that are compatible with viability and a low-growth phenotype (30). To further explore the essentiality of the *esaSR* locus, we set out to perform gene deletion experiments. We first attempted deletion of the complete *esaSR* locus with a mutagenesis system that uses the homing endonuclease I-SceI (31). First, we delivered a suicide plasmid carrying a trimethoprim (TMP) resistance cassette, the flanking regions of *esaSR*, and the I-SceI recognition site to *B. cenocepacia* K56-2, resulting in TMP-resistant transformants arising from the plasmid-targeted insertion into the chromosome via a first event of homologous recombination. Next, we introduced the plasmid pDAI-SceI, which constitutively expresses the I-SceI nuclease and contains a TET resistance cassette. I-SceI causes a double-strand break in the inserted plasmid sequence, which stimulates intramolecular recombination. The resolution of this cointegrate can either restore a wild-type configuration or cause a gene deletion, depending on the site of the crossover. This second event of recombination can be selected by screening colonies for TMP susceptibility, which corresponds to loss of the antibiotic resistance marker. Typically, 50% of the TMP-sensitive screened colonies harbor the deletion genotype, which can then be confirmed by colony PCR

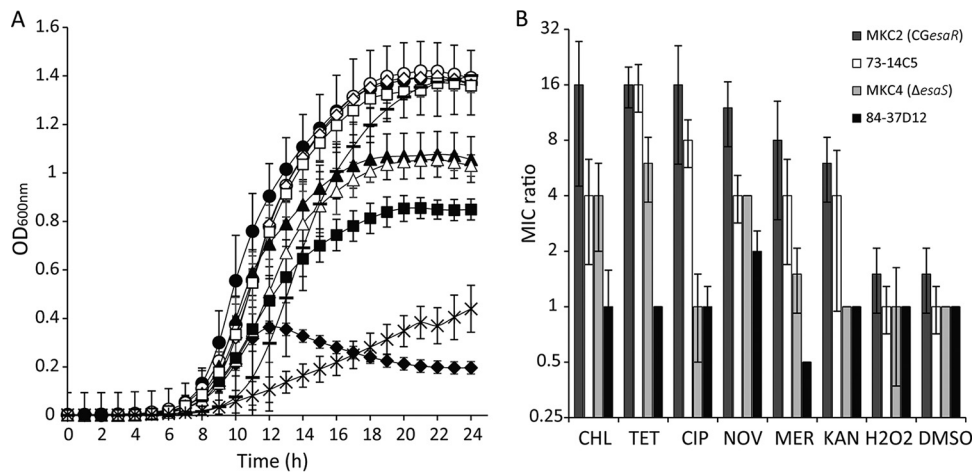


**FIG 5** Depletion of *EsaR* and *EsaS* causes a growth defect and lower MICs of select antibiotics. (A) Growth curves of strains grown in LB in the presence and absence of rhamnose. *B. cenocepacia* K56-2 wild type, ○, rhamnose, ●, no rhamnose; 73-14C5 (CG transposon mutant of *esaR*), □, rhamnose, ■, no rhamnose; MKC2 (CGesaR), ◇, rhamnose, ◆, no rhamnose; MKC4 ( $\Delta$ *esaS*), △, rhamnose, ▲, no rhamnose; and 84-37D12, –, rhamnose, ×, no rhamnose. The error bars represent the standard deviations of the results of at least two independent experiments. (B) MIC ratios of MKC2 (CGesaR), MKC4 ( $\Delta$ *esaS*), 73-14C5 (CG transposon mutant of *esaR*), and 84-37D12 (CG transposon mutant unrelated to *esaR*) in response to CHL, TET, CIP, NOV, KAN, MER, DMSO, and H<sub>2</sub>O<sub>2</sub>. The MIC ratio was calculated as the MIC of the mutant divided by the MIC of the wild type in the absence of rhamnose. The MICs used for the MIC ratio calculation are listed in Table 3. The median MIC ratios and standard deviations of the results of at least three independent experiments are shown.

using appropriate primers. We reasoned that if *esaR* was essential, resolution of the cointegrate would result in 100% wild-type configurations. Two consecutive attempts to delete *esaSR* resulted in 100% wild-type configurations. We then attempted to delete the *esaSR* locus for a third time while simultaneously attempting to delete only *esaS*. After the first event of recombination and for each deletion experiment, 24 TMP-resistant colonies harboring pDAI-Scel were grown in the absence of TMP and screened for loss of the TMP resistance phenotype. Fifteen and seven colonies were found to be TMP susceptible for the *esaS* and the *esaSR* locus deletion attempts, respectively. Of those, two colonies were found to have a deletion of the *esaS* gene (see Fig. S4 in the supplemental material). In contrast, all the colonies corresponding to the *esaSR* deletion attempt had reverted to the wild-type configuration. The success in obtaining an unmarked deletion of the histidine kinase gene, *esaS*, but not of the whole TCS locus, *esaSR*, confirms that *esaS* is dispensable and strongly suggests that *esaR* is essential for growth. The *esaS* gene deletion mutant ( $\Delta$ *esaS*) was named MKC4 and selected for further phenotypic analysis. To investigate the phenotype caused by depletion of *esaR*, we placed the rhamnose-inducible promoter upstream of *esaR* by site-directed mutagenesis, leaving intact the *esaS* locus. This new CG mutant was called MKC2 (CGesaR). In the absence of rhamnose, MKC2 showed a more severe growth defect than 73-14C5, while MKC4 displayed a moderate growth defect, intermediate between 73-14C5 and the wild type (Fig. 5A).

#### The *esaSR* locus is involved in drug efflux activity and cell membrane integrity.

To confirm that the *esaSR* locus is related to antibiotic resistance in *B. cenocepacia*, we determined antibiotic MICs against *B. cenocepacia* K56-2 wild type, MKC2 (CGesaR), MKC4 ( $\Delta$ *esaS*), and 73-14C5 (Table 3). Since MKC2 (CGesaR) has a pronounced growth defect, a CG mutant, 83-37D12, that has a growth defect similar to that of MKC2 (CGesaR) in the absence of rhamnose was included in the assay (Fig. 5) (26). In 84-37D12, the rhamnose-inducible promoter controls the expression of four genes, BURCENK562V\_RS02270, BURCENK562V\_RS02265, BURCENK562V\_RS02260, and BURCENK562V\_RS02255, that are predicted to be in an operon (32) and involved in purine metabolism (33). The MIC ratios, calculated as the fold change in the MIC for the wild type with respect to that of each mutant grown without rhamnose (Fig. 5B),



**TABLE 3** MICs of select antibiotics against *B. cenocepacia* K56-2 WT, MKC2 (*CGesaR*), MKC4 ( $\Delta$ *esaS*), 73-14C5 (CG transposon mutant of *esaR*), and 86-37D12 (CG transposon mutant unrelated to *esaR*)

Drug <sup>a</sup>	MIC <sup>b</sup>									
	WT		MKC4 ( $\Delta$ <i>esaS</i> )		MKC2 ( <i>CGesaR</i> )		73-14C5		84-37D12	
	(no rha)	(no rha)	No rha	Rha	No rha	Rha	No rha	Rha	No rha	Rha
CHL	16	4	1	16	4	16	16	32		
TET	8	1.5	0.75	4	0.5	8	8	8		
CIP	2	2	0.125	3	0.25	2	2	2		
NOV	8	2	1	12	4	2	8	8		
MER	32	24	4	48	8	8	64	64		
KAN	1,000	1,000	187.5	1,000	250	1,000	1,000	1,000		
H <sub>2</sub> O <sub>2</sub>	0.1875	0.234375	0.140625	0.28125	0.1875	0.1875	0.1875	0.1875		
DMSO	12.5	12.5	9.375	12.5	12.5	12.5	12.5	12.5		

<sup>a</sup>CIP, ciprofloxacin; MER, meropenem.

<sup>b</sup>Median MICs (micrograms per milliliter, except H<sub>2</sub>O<sub>2</sub> [millimolar] and DMSO [percent {vol/vol}]) from three independent experiments; rha, rhamnose.

were in agreement with the antibiotic sensitivity profile of 73-14C5 in the ESA (Fig. 4). Both mutants in which the rhamnose-inducible promoter controls the expression of *esaR* showed at least a 4-fold decrease in the MICs of chloramphenicol, tetracycline, ciprofloxacin, novobiocin, and meropenem in the absence of rhamnose. The mutant unrelated to MKC2 but possessing a similar growth defect, 84-37D12, did not show the same level of sensitivity as the *esaR*-depleted strains. This result, in concordance with the antibiotic sensitivity of the *EsaR*-depleted mutant, 73-14C5, which does not have a severe growth defect, indicates that the increased MIC ratio for MKC2 (*CGesaR*) is not an effect of the lack of growth. MKC4 ( $\Delta$ *esaS*) showed at least 4-fold chloramphenicol, tetracycline, and novobiocin MIC ratios, but not of the other antibiotics tested. None of the *esa* mutants showed this increased level of sensitivity to DMSO or hydrogen peroxide compared to the wild type (Fig. 5B and Table 3). Since the *esaR* and *esaS* mutants were sensitive to different classes of antibiotics, we investigated whether mutation at these loci causes a lack of efflux, resulting in the increased sensitivity to antibiotics. Efflux activity was assessed by measuring the fluorescence from  $\beta$ -naphthylamine, which is the cleavage product produced immediately upon the uptake of L-alanine  $\beta$ -naphthylamide (Ala-Nap) into the cell (34). As Ala-Nap is known to be a substrate of the MexAB-OprM efflux pump of *Pseudomonas aeruginosa* and the AcrAB-TolC pump of *Escherichia coli*, an increase in fluorescence indicates inhibition of efflux activity (34). Mutants 73-14C5 and MKC2 (*CGesaR*) had approximately 8- and 3-fold increases in fluorescence, respectively, compared to the wild type at the 1-hour time point of the assay (Fig. 6A). This increase in fluorescence over time was observed for 73-14C5 and MKC2 (*CGesaR*) when grown overnight without rhamnose. When grown in the presence of rhamnose to induce expression of *esaR*, the level of fluorescence produced by 73-14C5 and MKC2 (*CGesaR*) was as low as that of the K56-2 wild type, indicating a role of *EsaR* in activating efflux or maintaining the integrity of the membrane (Fig. 6A). The effect of deleting *esaS* was not as strong, as MKC4 ( $\Delta$ *esaS*) displayed only a 1.5-fold increase in fluorescence compared to the wild type.

In an effort to induce efflux prior to the Ala-Nap uptake assay, we pretreated the cells with chloramphenicol for 3 h in the absence of rhamnose. Similar to the results shown in Fig. 6A, untreated 73-14C5 and MKC2 (*CGesaR*), but not MKC4 ( $\Delta$ *esaS*), observed an increase in fluorescence relative to that of wild-type cells (Fig. 6B), and the difference was statistically significant (WT versus 73-14C5,  $P < 0.01$ ; WT versus MKC2,  $P < 0.05$ ). Chloramphenicol caused a decrease in the fluorescence of the wild-type cells compared to the nonantibiotic control (WT without CHL versus WT plus CHL,  $P < 0.001$ ), suggesting that chloramphenicol induced efflux. In agreement with a role of *esaS* in chloramphenicol-mediated induction of efflux, MKC4 ( $\Delta$ *esaS*) did not show any decrease in fluorescence in the presence of chloramphenicol. On the contrary, fluores-

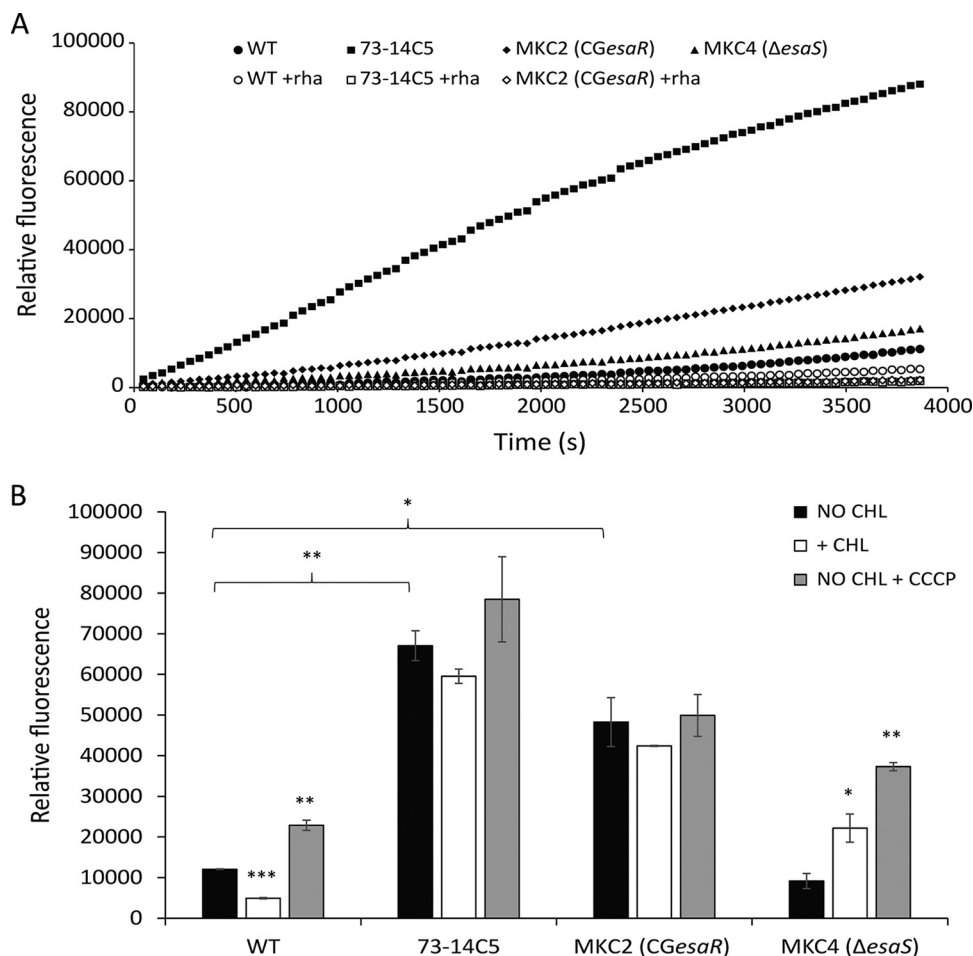


**FIG 6** Efflux activities of *B. cenocepacia* K56-2 WT, 73-14C5 (CG transposon mutant of *esaR*), MKC2 (*CGesaR*), and MKC4 ( $\Delta$ *esaS*). Efflux activity was assessed by measuring the relative fluorescence produced by cultures treated with Ala-Nap. The rate of uptake of nonfluorescent Ala-Nap and immediate cleavage to fluorescent  $\beta$ -naphthylamine are indicative of the efflux activity of the cell. (A) Relative fluorescence values of cultures over time when grown overnight in the presence (open symbols) and absence (solid symbols) of rhamnose (rha). The results shown are representative of three independent experiments. (B) Relative fluorescence values of chloramphenicol-treated and untreated cultures at the 1-h time point of the Ala-Nap assay. Cultures grown overnight without rhamnose were adjusted to an OD<sub>600</sub> of 1.0 and incubated in the absence (black bars) or in the presence (white bars) of CHL for 3 h prior to the Ala-Nap assay. Ten minutes into the assay, 10  $\mu$ M CCCP was added to the cells to disrupt efflux (gray bars). The error bars represent the standard deviations of two biological replicates. A *t* test was performed with GraphPad software to determine significant differences. \*,  $P < 0.05$ ; \*\*,  $P < 0.01$ ; \*\*\*,  $P < 0.001$ .

cence increased nearly 2-fold compared to the no-chloramphenicol condition ( $P < 0.05$ ) (Fig. 6B). There were no significant differences between untreated and chloramphenicol-treated cells when they were depleted of *esaR* (73-14C5 and MKC2). Treatment of wild-type cells with the proton gradient-uncoupling agent CCCP significantly inhibited efflux in wild-type (WT versus WT with CCCP,  $P < 0.01$ ) and  $\Delta$ *esaS* (MKC4 versus MKC4 plus CCCP,  $P < 0.01$ ) cells but did not result in a significant increase in fluorescence in the *EsaR*-depleted mutants.

Differential interference contrast (DIC) microscopy imaging was used to further characterize the phenotypes of *EsaS*- and *EsaR*-depleted cells. After 24 h of growth in the presence of rhamnose, MKC2 (*CGesaR*) and 84-37D12 showed rod-shaped morphology, similar to the wild-type phenotype (see Fig. S7 in the supplemental material). All of the *EsaR*-depleted MKC2 (*CGesaR*) cells examined were small, spherical cells, while MKC4 ( $\Delta$ *esaS*) and 84-37D12 cells had rod shapes more similar to that of the wild type when grown for 24 h without rhamnose (Fig. 7). In the Ala-Nap assay, the strong fluorescent signal and lack of chloramphenicol-induced efflux in MKC2 (*CGesaR*) and

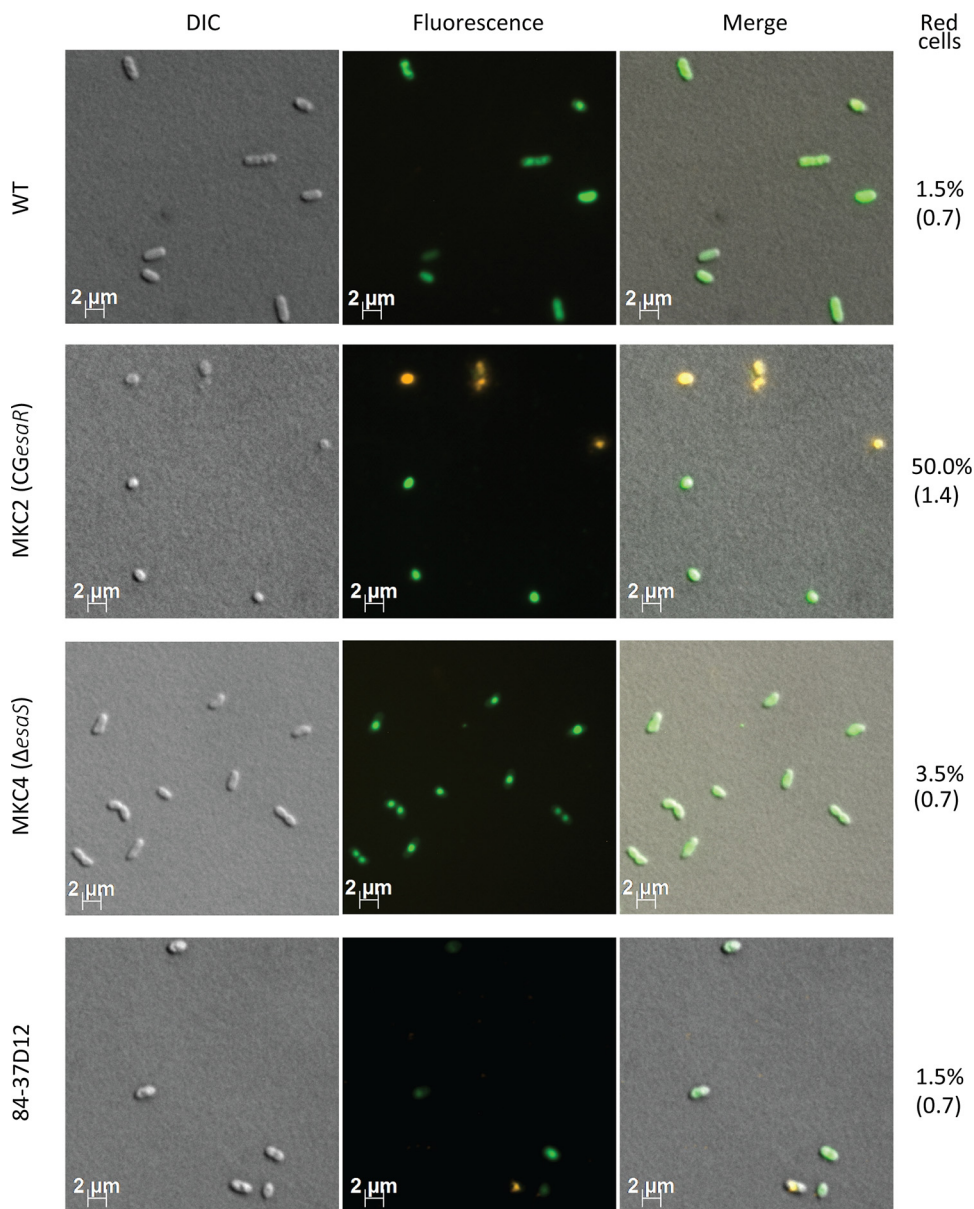


**FIG 7** *B. cenocepacia* cells have a compromised membrane when depleted in EsaR. Cultures of WT, MKC2 (CGesaR), MKC4 ( $\Delta$ esaS), and 84-37D12 (CG mutant unrelated to *esaR*), incubated for 24 h in the absence of rhamnose, were stained with SYTO9 and PI from the BacLight LIVE/DEAD bacterial viability kit (Molecular Probes) and visualized by fluorescence microscopy. Fluorescent green bacteria indicate intact membranes, while fluorescent red cells represent bacteria with compromised membranes. The average percentage of fluorescent red cells and standard deviations (in parentheses) from two independent experiments are shown.

73-14C5 raised the question of whether efflux is solely responsible for the increased uptake of Ala-Nap or if the lack of EsaR also compromises the cell membrane. To explore the membrane integrity of *esaR*-depleted cells, we examined microscopy images of cells stained with the fluorophores SYTO9 and propidium iodide (PI). SYTO9 is a green-fluorescent nucleic acid stain capable of passing through intact membranes, while PI is a hydrophobic red-fluorescent nucleic acid stain that stains only cells with compromised membranes. PI staining was observed in 50% of the EsaR-depleted MKC2 (CGesaR) cells, indicating that EsaR-depleted cells have compromised membranes (Fig. 7). The other strains examined had intact cell membranes, as less than 4% of WT, MKC4 ( $\Delta$ esaS), and 84-37D12 cells were stained with PI (Fig. 7). Together with the increased MIC ratios of 73-14C5, MKC2 (CGesaR), and MKC4 ( $\Delta$ esaS) combined with the increased

Ala-Nap uptake in *esaR*-depleted cells and *esaS*-depleted cells treated with chloramphenicol, our results strongly suggest that the *B. cenocepacia* *esaSR* two-component system regulates resistance to antibiotics by maintaining cell envelope integrity and through efflux activity.

## DISCUSSION

In this work, we identified and characterized a two-component system as a promising antibiotic target for Bcc infections. We used a pilot CG library underexpressing essential genes, grown competitively in a pool, and quantified their relative abundances using next-generation sequencing. The pilot CG library included a *gyrB* CG mutant (*CGgyrB*) previously shown to have enhanced sensitivity in the presence of sublethal concentrations of novobiocin, when measured by OD<sub>600</sub> (26). Growing CG mutants together in the competitive ESA magnified the level of enhanced sensitivity of *CGgyrB* to novobiocin (Fig. 3). We consider pooled growth to be more advantageous than clonal growth, as it reduces the amounts of reagents required—notably, the amount of compound needed—and does not require specialized robotic equipment or imaging software. Tracking the relative abundances of competitively grown mutants by Illumina sequencing increases the dynamic range of sensitization detection compared to measuring mutant growth by OD<sub>600</sub>. In any assay, expanding the signal window allows more accurate discrimination of signal from noise. The ability to generate a strong signal using a low dose of compound is significant because using higher doses of compound can have an obscuring effect, as it increases the signal of not only the strain underexpressing the target, but all the strains, due to nonspecific toxicity. The increased hypersensitivity from competitive growth that we observed, coupled with the nearly unlimited dynamic range of detection of Illumina sequencing, shows promise for the method to generate detailed mutant profiles. The identification of both strongly and moderately sensitized mutants creates profiles for novel compounds that can inform genes capable of buffering compound activity and in turn facilitate rational drug design and point to potential combination therapies. Another reason for generating comprehensive mutant profiles to determine MOA is that, while depletion of the antimicrobial target is likely to have the strongest signal, this is not always the case. A contrary example is aminoglycosides, where the mutant profiles show that the mechanism of killing is similar to that of membrane-disrupting antibiotics (35) and does not reflect its target, the ribosome (36). In addition to novobiocin, *CGgyrB* showed marginally enhanced sensitivity to tetracycline (IC<sub>10</sub> and IC<sub>30</sub>) and colistin (IC<sub>30</sub>), which highlights the complexity of sensitization profiles for compounds, even when the compounds are associated with a single target. A likely explanation is that the hypersensitivity of nontarget CG mutants to a compound may be observed when there is an associated cellular process involved. Donald et al. (35) reported that a GyrB-depleted strain of *Staphylococcus aureus* showed enhanced sensitivity to daunorubicin, a tetracycline-like compound. While inhibition of DNA gyrase activity interferes with DNA replication (37, 38), daunorubicin intercalates within DNA and causes DNA fragmentation and single-strand breaks (39). Therefore, inhibition of DNA replication may sensitize *S. aureus* to daunorubicin. Underexpression of *gyrB* sensitizes *B. cenocepacia* (this study) and *S. aureus* (35) to tetracycline. Despite the ribosome being the primary target of tetracycline (40), tetracycline can also bind and introduce damage to DNA, which is enhanced by the formation of metal complexes (41, 42). GyrB depletion also sensitized *B. cenocepacia* to colistin, although the effect was observed only with colistin at the IC<sub>30</sub>. Colistin is a polypeptide antibiotic of the polymyxin family that targets the cell membrane through initial interaction with the lipopolysaccharide portion of the outer membrane (43). While the reasons for the marginally enhanced sensitivity of the *B. cenocepacia* *CGgyrB* mutant to colistin are not known, a likely explanation is that both inhibition of DNA replication by *gyrB* depletion and the action of colistin increase the production of reactive oxygen species (ROS), contributing to the sensitization mechanism. Although there are no data available for novobiocin- or colistin-mediated ROS production, the fluoroquinolone moxifloxacin, at a concentration that inhibits the

DNA gyrase, induced the production of hydroxyl radical (44). Similarly, polymyxin B was shown to kill *Acinetobacter baumannii* by hydroxyl radical production (45). In addition to identifying the drug binding targets, the increased signal in the competitive enhanced-sensitivity assay facilitates the identification of subtle interactions of affected pathways by generating an intricate CG mutant profile for each antibiotic to determine the MOA of novel antibiotics. These detailed mutant profiles can provide a tool to direct chemical engineering during compound optimization.

While we were able to reliably quantify the relative abundances of the CG mutants in the pilot CG library, using a single multiplex PCR restricted the number of strains we were able to screen, which is a limitation of the assay. No correlation was found between the amplicon size, thermodynamic properties of the primers or amplicons, and relative detection or amplification variability of the CG mutants (data not shown). However, it is possible to include more CG mutants using a manifold of individually optimized multiplex PCRs, as was done previously (35). Creating amplicons by other methods, such as the Tn-seq circle (46), or using barcoded transposons, as in RB-TnSeq (47) or TagModules (48), which do not require the use of multiplex PCR primers, would be more amenable to the addition of new strains in the ESA, since they do not require previous knowledge of transposon insertion sites or optimization of multiplex PCRs. This would be advantageous, since profiling more strains through the ESA would increase the likelihood of matching novel growth inhibitors to their targets.

Profiling the sensitivities of the CG mutants to several antibiotics uncovered a CG mutant of a TCS that was hypersensitive to several classes of antibiotics. This putative TCS (*EsaSR*) is encoded by BURCENK56V\_RS04770 and BURCENK56V\_RS04765, which likely form an operon. The *B. cenocepacia* K56-2 *esaSR* genes are homologous to the BCAL0471-BCAL0472 genes, which have also been annotated as forming a putative TCS in the *B. cenocepacia* J2315 genome (33). Remarkably, the BCAL0471-BCAL0472 locus is just 1 of more than 40 TCSs that remain uncharacterized in *B. cenocepacia* genomes. TCSs are used by bacteria to sense environmental stimuli through a membrane-bound histidine kinase that activates a cytoplasmic response regulator that in turn mediates changes in gene expression (49). Many TCSs have been implicated in the regulation of antibiotic resistance (50–52) through the overexpression of efflux pumps (53–58) or maintaining cell membrane integrity (59–62). Outer membrane permeability and efflux activity are synergistic processes that are often associated (63). Reactive oxygen and nitrogen species are known to induce expression of efflux pumps through activation of TCSs (64–66), and outer membrane permeability can be regulated in response to oxidative stress (67). It is notable that the sensor histidine kinase (BURCENK56V\_RS04770) contains a PAS domain, which is used to sense the redox state of the cell in many prokaryotes (68).

Genetic analysis of the *esaSR* locus strongly suggests that *esaR* is an essential gene. Gene essentiality is challenging to demonstrate experimentally. Systems in which a gene is deleted in the presence of a second copy expressed from a plasmid are available for some bacteria (69). In those cases, plasmid maintenance in the absence of selection is deemed to be a confirmation of gene essentiality (70). The limited availability of genetic tools for *B. cenocepacia* precluded us from using this approach. However, we demonstrated that although the first event of homologous recombination directed at mutagenizing *esaR* was achieved, resolution of the cointegrate in the merodiploids always produced excision of the integrated plasmid with reversion to the wild-type conformation. In contrast, parallel experiments aimed at deleting *esaS* resulted in *esaS* deletion mutants. This observation strongly suggests that while *esaS* is dispensable, *esaR* is not. In support of this, a recent high-density transposon mutagenesis study in *B. cenocepacia* J2315 did not identify any mutants with insertions in the homolog of *esaR*, BCAL0472, indicating that it is essential, while mutants with insertions that disrupted *esaS* were recovered (71). A few essential TCSs with a regulatory role in cell wall homeostasis have been described (62, 72). The *S. aureus* WalkR system is remarkable in that temperature-sensitive mutants are also hypersusceptible to antibiotics (73). It is possible, then, that the essentiality of *B. cenocepacia* *esaR* is related to a

similar role, controlling cell envelope processes. We have demonstrated that depletion of *esaS* or *esaR* also results in an increase of fluorescence during the Ala-Nap uptake assay, which suggests reduced efflux of the Ala-Nap reagent. However, to expose the involvement of *esaS* in activating efflux, previous treatment with chloramphenicol was necessary (Fig. 6B). Instead, depletion of *EsaR* increases Ala-Nap uptake regardless of previous induction with chloramphenicol, indicating that *esaS* and *esaR* can regulate different processes, efflux and membrane integrity. The lack of increased Ala-Nap uptake by both the CCCP-treated MKC2 (*CGesaR*) and 73-14C5 suggests that depletion of *esaR* causes either a comprehensive shutdown of efflux or an increase in the permeability of the membrane. The fact that 73-14C5 was hypersensitive to CCCP supports the latter explanation, since a cell with an unstable membrane would be more susceptible to disruption of the proton motive force. The results from the Ala-Nap uptake assay are consistent with the microscopy images showing that MKC2 (*CGesaR*) has a compromised membrane, while the lack of PI staining in MKC4 ( $\Delta$ *esaS*) indicates an intact membrane. Importantly, while the differential staining by STYO9 and PI is conventionally used to assess cell viability, cells stained with PI may be viable (74).

It is tempting to speculate that *EsaS*-dependent phosphorylated *EsaR* activates efflux pump genes but unphosphorylated *EsaR* is capable of regulating cell envelope processes. Therefore, while *esaS* seems to regulate antibiotic-induced efflux, it remains to be demonstrated to what extent the role of *esaR* is related to regulation of efflux pumps, cell envelope homeostasis, or a contribution of both mechanisms.

Much interest has been focused on TCSs as valuable drug targets due to the fact that TCSs are not present in humans and targeting them could reduce virulence (75, 76) and antibiotic resistance (76). Inhibitors of a TCS involved in antibiotic resistance could provide effective therapies for treating infections by multidrug-resistant bacteria, in combination with antibiotics. A TCS that mediates resistance to different antibiotics represents a lucrative target in *B. cenocepacia* for combatting antibiotic resistance, since inhibitors of the TCS could render the strain susceptible to antibiotics currently in use.

## MATERIALS AND METHODS

**Bacterial strains and growth conditions.** Fifty-six strains (see Table S1 in the supplemental material) from a library of *B. cenocepacia* K56-2 CG mutants (26, 27) were used. All the strains were cultured in Luria Bertani (LB) medium (Difco, Becton, Dickinson and Company, Sparks, MD, USA) supplemented as required with 100  $\mu$ g/ml TMP and different inducing concentrations of rhamnose with shaking at 37°C. Standardized glycerol stocks of *B. cenocepacia* K56-2 (wild type) or CG mutants within the same rhamnose category pooled in equal amounts were prepared as previously described (26). For growth in 96-well plates, glycerol stocks were thawed, inoculated at a final optical density ( $OD_{600}$ ) of 0.001 in a total volume of 200  $\mu$ l, and incubated at 37°C with shaking at 220 rpm for 22 h. Growth ( $OD_{600}$ ) was measured using a BioTek Synergy 2 plate reader (BioTek Instruments, Inc., Winooski, VT, USA).

**Growth inhibitors.** All chemicals were purchased from Sigma-Aldrich (St. Louis, MO) unless otherwise indicated. NOV, CHL, TET, KAN, COL, CCCP, H<sub>2</sub>O<sub>2</sub>, and DMSO were supplemented at IC<sub>10</sub>s and IC<sub>30</sub>s for wild-type growth. To calculate the IC<sub>10</sub> and IC<sub>30</sub>, standardized glycerol stocks of *B. cenocepacia* K56-2 were inoculated in 96-well plates with and without a 2-fold dilution series of each antibiotic. After incubation, growth was measured by  $OD_{600}$  and the inhibitory concentrations were predicted by nonlinear regression analysis by fitting the log<sub>10</sub> (inhibitor)  $OD_{600}$  readings to the Hill equation using GraphPad Prism (GraphPad Software Inc., La Jolla, CA).

**Multiplex PCR optimization, amplicon library preparation, and Illumina sequencing of amplicons.** A multiplex primer set was designed (77), consisting of a common transposon-specific forward primer and genome-specific reverse primers (see Table S2 in the supplemental material), to amplify the transposon-genome interface of each CG mutant (see Table S1 in the supplemental material) in a multiplex PCR (Fig. 1). The starting template concentration and number of cycles that produced exponential amplification of the amplicon pool was determined by quantitative PCR (qPCR) using IQ SYBR green Supermix (Bio-Rad) in a Bio-Rad IQ5 thermocycler (Bio-Rad, Hercules, CA, USA). Since the qPCR showed the average amplification of all the amplicons, next-generation sequencing was used to determine the amplification reproducibility of the individual CG mutants. Each 100- $\mu$ l multiplex PCR used 20 ng of genomic DNA template, IQ Supermix (Bio-Rad, Hercules, CA, USA), and individual primer concentrations adjusted to achieve reproducible amplification of each CG mutant (see Table S2 in the supplemental material). The reactions were done in an Eppendorf Mastercycler ep gradient S thermal cycler (Eppendorf Canada Ltd., Mississauga, ON, Canada) using 5 min of denaturation at 95°C and 27 cycles of denaturation at 95°C for 30 s, annealing at 67°C for 30 s, and extension at 72°C for 30 s, followed by a final extension at 72°C for 10 min. Amplicons created in the multiplex PCR containing the transposon-genome interface were size selected using Agencourt AMPure XP beads (Beckman Coulter, Brea, CA, USA) and used as the template for the indexing PCR. To identify amplicons created using

different primer concentrations, indexing primers containing 5' adapters with the index sequences and Illumina MiSeq-specific adapter sequences (Nextera Index kit; Illumina Inc., San Diego, CA) were added to the amplicons under PCR conditions recommended by the manufacturer. The amplicons were sequenced on an Illumina MiSeq (Illumina Inc., San Diego, CA) platform at the Children's Hospital Research Institute of Manitoba (Winnipeg, Canada) using either a micro- or standard flow cell, following the manufacturer's instructions.

**Data analysis.** We previously determined the locations of the insertion sites of the CG mutants by sequencing the transposon-genome interface of each CG mutant and aligning the resulting read against the genome of *B. cenocepacia* J2315 (26). This information was used to create a file containing the genomic portions of the amplicon sequences for each CG mutant. Demultiplexed fastq files obtained from sequencing were converted to fasta using prinseq-lite version 0.20.3 (78). The sequences in the forward-read fasta files were filtered to include only the reads containing the transposon sequence and aligned with the amplicon sequences of the CG mutants using a standalone version of BLASTn from NCBI (79). The amplicon count from BLASTn was converted to tabular format using the command line outfmt 6. For determining amplicon read counts, sequences with more than 90% identity, at least 45-base alignment to an amplicon in the BLAST library, and a transposon score greater than 39 were included in the analysis. For the antibiotic and no-antibiotic (control) treatments, reads corresponding to a CG mutant were normalized as the RA of the total reads per index (treatment). CG mutant depletion ratios in response to an antibiotic ( $DR_{\text{antibiotic}}$ ) were calculated as a  $\log_{10}$  of the mean  $RA_{\text{control}}$  divided by the  $RA_{\text{antibiotic}}$ . To determine the significance of depletion, Z scores were calculated using error models ( $DR_{\text{control}}$ ) generated for each mutant from replicate controls:  $Z = (DR_{\text{antibiotic}} - \text{mean } DR_{\text{control}}) / (\text{mean } |DR_{\text{antibiotic}} - \text{mean } DR_{\text{control}}|)$ .

CG mutants with  $\log_2$  depletion ratios and Z scores greater than 2 were deemed significantly depleted under a given condition.

**Artificial depletion of CG mutants.** Pools of CG mutants were created from the pilot CG library by growing the selected strains clonally and then combining them in specific ratios based on their  $OD_{600}$ . CG mutants were combined in equal amounts (pool A), and four depletion pools were generated from the same clonally grown strains, with selected mutants depleted by 10-fold or 100-fold (pools B, C, D, and E), in comparison with the library pooled in equal amounts. The transposon-genome interface of the CG mutants in each pool was then amplified by two-step PCR and sequenced in parallel on the Illumina MiSeq. Depletion of each CG mutant was assessed by comparing the percent abundance of each mutant in the depleted pool to the percent abundance of CG mutants pooled in equal amounts.

**Competitive enhanced-sensitivity assay.** Each CG mutant of the pilot CG library was categorized into rhamnose categories based on similar growth phenotypes in response to rhamnose, as described previously (26). CG mutants that reached 30 to 60% of wild-type growth at a given rhamnose concentration were combined for growth in pools (see Fig. S1 in the supplemental material). For the assay, standardized glycerol stocks containing CG mutants pooled in equal amounts were thawed and inoculated at a final  $OD_{600}$  of 0.001 in 96-well plates with the chosen rhamnose concentrations and antibiotics. After incubation for 22 h with shaking at 220 rpm, equal volumes of mutant pools exposed to the same treatment were combined, and the genomic DNA of each library was extracted. Amplicon libraries of the CG mutant transposon-genome interfaces were prepared by two-step PCR. First, adaptors were added by a multiplex PCR that uses a common transposon-specific forward primer and a genome-specific reverse primer, both of which contain 5' adapter sequences. Then, an index PCR added indexes to the amplicons using primers complementary to the adapter sequences and containing 5' indexes and Illumina MiSeq-specific adapter sequences. Each unique index identified the treatment each library was exposed to (control or antibiotic). Amplicon libraries were sequenced in parallel on the Illumina MiSeq as described above.

**Comparison of pooled and clonal growth.** Standardized glycerol stocks of CG mutants (58-14E1, 67-5H10, 86-3D16, and 96-1K12), individually or pooled in equal amounts, from the same rhamnose group (see Fig. S1 and S4 in the supplemental material) were inoculated at a final  $OD_{600}$  of 0.001 and grown clonally or in a pool in the presence or absence of novobiocin and chloramphenicol at their  $IC_{10\%}$ . After incubation, genomic DNA of the cocultured CG mutants was isolated directly, while the  $OD_{600}$  of the clonally grown strains was measured, and then equal volumes of each strain were pooled before extracting the genomic DNA. Indexed amplicon libraries were produced from each condition and sequenced on the Illumina MiSeq. To compare the relative abundances of each mutant between treatment conditions, amplicon reads were normalized by dividing the number of reads from each CG mutant amplicon by the total number of reads for one condition. Fold depletion was determined by dividing the normalized reads for each CG mutant under the no-antibiotic condition by the normalized reads from each CG mutant under the antibiotic condition. As a control, the depletion ratios of pooled growth and clonal growth were compared for each CG mutant under the no-antibiotic condition by dividing normalized reads for each CG mutant grown in a pool by the normalized reads from each CG mutant grown clonally.

**Construction of the unmarked *esaS* deletion mutant, MKC4 ( $\Delta$ esaS).** An unmarked deletion of *esaS* (BURCENK56V\_RS04770) in *B. cenocepacia* K56-2 was produced as described by Flannagan et al. (31). Primers 666 (5'-AGATAATCTAGAGACTTCGAGCTGAATCCGA) and 665 (5'-ATATGGATCCGTCGGTCACCGTGAAG) were used to amplify a 450-bp fragment upstream of *esaS*. Primers 664 (5'-ATATGGATCCCAAAGGCAGCGTAAATGGCA) and 663 (5'-AATTATCCCGGGCTTGAGCTTGCGATACAG) were used to amplify a 450-bp region downstream of *esaS*. These amplicons were digested with BamHI (New England Biolabs Inc., Ipswich, MA, USA) and ligated with T4 DNA ligase (New England Biolabs Inc., Ipswich, MA, USA). The resulting DNA fragment was digested with XbaI and XmaI (New England Biolabs Inc., Ipswich, MA, USA)

and ligated into the XbaI- and XmaI-digested pGPI-SceI to create plasmid pMC4. To attempt deletion of the *esaSR* locus, a 925-bp DNA fragment consisting of 450-bp regions upstream and downstream of *esaSR* was synthesized by Blue Heron Biotech, digested with XbaI and XmaI, and ligated into the XbaI- and XmaI-digested pGPI-SceI to create plasmid pMC5. pMC4 and pMC5 were conjugated into *B. cenocepacia* K56-2, and merodiploids were selected on LB agar plates supplemented with 100  $\mu\text{g/ml}$  TMP and 50  $\mu\text{g/ml}$  gentamicin. To initiate the second recombination event, pDAI-SceI, which carries the yeast homing endonuclease I-SceI coding gene, was introduced by triparental mating into TMP-resistant clones. Tetracycline-resistant clones were screened for the loss of TMP resistance, and the recovered TMP-susceptible clones were screened by colony PCR to isolate deletion mutants. To identify the deletions of *esaS* and *esaSR*, primers 615 (5'-AATTAACATATGGTGATCGTCTCGACCGTGG) and 616 (5'-ATA TAATCTAGAGATGTAGATGATCCCGCCCG), which amplify 270 bp corresponding to the 5' end of *esaS*, were used, as well as primers 666 and 663, which amplify *esaS* with flanking 500-bp segments upstream and downstream of the gene (see Fig. S4 in the supplemental material). Confirmed deletion mutants were passaged in LB broth over a period of 9 days to cure colonies of pDAI-SceI, and selection was done by replica plating on LB agar plates and LB agar plates supplemented with 100  $\mu\text{g/ml}$  tetracycline.

#### Site-directed mutagenesis to construct the *esaR* conditional growth mutant MKC2 (CGesAR).

The 5' end (170 bp) of *esaR* was amplified via PCR using HotStar HiFidelity polymerase (Qiagen, Hilden, Germany) with primers 633 (5'-AATTAACATATGATGGCAACCATCTGGTG) and 634 (5'-ATATAATCTAGACATTCCTTGAGCAGCGTGAC), digested with NdeI and XbaI (New England BioLabs Inc., Ipswich, MA, USA), and cloned into pSC201 immediately downstream of the rhamnose-inducible promoter. The resulting mutagenesis plasmid, pMC2, was introduced into *B. cenocepacia* K56-2 by triparental mating (80). Exconjugants were selected on LB agar plates supplemented with 0.2% rhamnose, 100  $\mu\text{g/ml}$  trimethoprim, and 50  $\mu\text{g/ml}$  gentamicin. Insertional mutants were confirmed by PCR using primer 645 (5'-GCCCCATTTCTCTGTAGTAACGAGA) and primer 652 (5'-GCATCCAGATATCGAGCAGCA), which anneal with pSC201 and a region downstream of the 170-bp 5'-end fragment of *esaR*, respectively.

**MIC ratios.** MIC assays were performed in *B. cenocepacia* K56-2 (wild type), 73-14C5 (CG transposon mutant of *esaR*), MKC2 (CGesAR), MKC4 (*DesaS*), and 84-37D12 (CG transposon mutant unrelated to *esaR*) in a final volume of 200  $\mu\text{l}$ . Standardized glycerol stocks were diluted to a final OD<sub>600</sub> of 0.001 in LB broth and added to 96-well plates containing 2-fold serial dilutions of the antibiotic to be tested. When required, rhamnose was added at a final concentration of 0.16% (wt/vol). The highest concentrations of antibiotics tested were as follows: novobiocin at 64  $\mu\text{g/ml}$ , ciprofloxacin at 64  $\mu\text{g/ml}$ , chloramphenicol at 64  $\mu\text{g/ml}$ , tetracycline at 64  $\mu\text{g/ml}$ , DMSO at 25% (vol/vol), kanamycin at 8 mg/ml, hydrogen peroxide at 3 mM, and meropenem at 64  $\mu\text{g/ml}$ . The plates were incubated for 22 h at 37°C without shaking. The MIC ratios were calculated for each strain as the MIC of the wild type divided by the MIC of the mutant, grown without rhamnose.

**Ala-Nap uptake assay.** Efflux activity was determined by measuring the amount of cleavage of Ala-Nap to fluorescent  $\beta$ -naphthylamine by bacterial cells as previously described (34, 81). Bacteria were grown overnight in LB or LB with 0.2% (wt/vol) rhamnose where indicated. The cultures were washed and resuspended in buffer solution (K<sub>2</sub>HPO<sub>4</sub> [50 mM], MgSO<sub>4</sub> [1 mM], and glucose [0.4%]) at pH 7.0. To initiate the reaction, 100- $\mu\text{l}$  cell suspensions at an OD<sub>600</sub> of 1.0 were treated with Ala-Nap at a final concentration of 128  $\mu\text{g/ml}$  in black, 96-well, flat-bottom plates (Corning Inc., Kennebunk, ME, USA). Fluorescence was measured every 45 s for 1 h on a BioTek Synergy 2 plate reader (BioTek Instruments Inc., Winooski, VT, USA) with excitation at 360 nm and emission at 460 nm. To induce efflux, cultures at an OD<sub>600</sub> of 1 were incubated in LB with 5  $\mu\text{g/ml}$  chloramphenicol for 3 h with shaking at 37°C. The cells were then washed, and the OD<sub>600</sub> was adjusted to 1 before performing the Ala-Nap uptake assay. For treatment with CCCP to inhibit active efflux, 10 min into the assay, CCCP was added at a final concentration of 10  $\mu\text{M}$ .

**Microscopy analysis.** Bacterial strains were inoculated into 5 ml of LB plus 0.2% rhamnose to a final OD<sub>600</sub> of 0.001 and incubated at 37°C with shaking at 220 rpm for 16 to 17 h. Fifteen microliters of each strain was then subcultured into 5 ml of LB or LB plus 0.2% rhamnose and incubated at 37°C with shaking at 220 rpm. After 24 h of incubation, the cultures were diluted 1 in 20 with phosphate-buffered saline (PBS) to prepare for staining using SYTO9 dye and PI from the BacLight LIVE/DEAD bacterial viability kit (Molecular Probes). Controls were set up using wild-type *B. cenocepacia* K56-2 added at a final 1/10 dilution to 4 ml PBS or 4 ml 70% isopropanol as the live and dead controls, respectively (see Fig. S6 in the supplemental material). The control tubes were incubated at room temperature for 1 h, with quick vortexing every 15 min. Diluted bacterial samples were stained with 3  $\mu\text{l}$  SYTO9 dye and PI staining solution for 15 min; 10  $\mu\text{l}$  of samples and controls was spotted onto 1% agarose-coated microscope slides and covered with coverslips. The slides were imaged using an AxioCamMR attached to an Axio Imager Z1 (Carl Zeiss) at  $\times 1,000$  magnification using DIC, rhodamine, and green fluorescent protein (GFP) fluorescence filters. To determine the proportion of cells with a compromised membrane, 100 fluorescent cells from each biological replicate were counted, and the average percentage of red cells and the standard deviation were reported.

## SUPPLEMENTAL MATERIAL

Supplemental material for this article may be found at <https://doi.org/10.1128/AAC.00790-16>.

**TEXT S1**, PDF file, 1.1 MB.



## ACKNOWLEDGMENTS

This work was supported by a research grant from Cystic Fibrosis Canada (CFC) to S.T.C. A.S.G. was supported by a Graduate Enhancement of the Tri-Council Stipend (GETS) from the University of Manitoba.

We are grateful to Deborah Tsuyuki for technical advice in regard to Illumina sequencing.

## REFERENCES

- Bush K, Courvalin P, Dantas G, Davies J, Eisenstein B, Huovinen P, Jacoby GA, Kishony R, Kreiswirth BN, Kutter E, Lerner SA, Levy S, Lewis K, Lomovskaya O, Miller JH, Mobashery S, Piddock LJ, Projan S, Thomas CM, Tomasz A, Tulkens PM, Walsh TR, Watson JD, Witkowski J, Witte W, Wright G, Yeh P, Zgurskaya HI. 2011. Tackling antibiotic resistance. *Nat Rev Microbiol* 9:894–896. <https://doi.org/10.1038/nrmicro2693>.
- Boucher HW, Talbot GH, Bradley JS, Edwards JE, Gilbert D, Rice LB, Scheld M, Spellberg B, Bartlett J. 2009. Bad bugs, no drugs: no ESCAPE! An update from the Infectious Diseases Society of America. *Clin Infect Dis* 48:1–12. <https://doi.org/10.1086/595011>.
- Mahenthalingam E, Urban TA, Goldberg JB. 2005. The multifarious, multireplicon *Burkholderia cepacia* complex. *Nat Rev Microbiol* 3:144–156. <https://doi.org/10.1038/nrmicro1085>.
- Burns JL. 2007. Antibiotic resistance of *Burkholderia* spp., p 81–91. In Coenye T, Vandamme P (ed), *Burkholderia*: molecular microbiology and genomics. Horizon Bioscience, Norfolk, VA.
- Beckman W, Lessie TG. 1979. Response of *Pseudomonas cepacia* to beta-lactam antibiotics: utilization of penicillin G as the carbon source. *J Bacteriol* 140:1126–1128.
- Gugliera P, Pasca MR, De Rossi E, Bironi S, Arrigo P, Manina G, Riccardi G. 2006. Efflux pump genes of the resistance-nodulation-division family in *Burkholderia cenocepacia* genome. *BMC Microbiol* 6:66. <https://doi.org/10.1186/1471-2180-6-66>.
- Zhou J, Chen Y, Tabibi S, Alba L, Garber E, Saiman L. 2007. Antimicrobial susceptibility and synergy studies of *Burkholderia cepacia* complex isolated from patients with cystic fibrosis. *Antimicrob Agents Chemother* 51:1085–1088. <https://doi.org/10.1128/AAC.00954-06>.
- Burdine L, Kodadek T. 2004. Target identification in chemical genetics: the (often) missing link. *Chem Biol* 11:593–597. <https://doi.org/10.1016/j.chembiol.2004.05.001>.
- Brown ED, Wright GD. 2005. New targets and screening approaches in antimicrobial drug discovery. *Chem Rev* 105:759–774. <https://doi.org/10.1021/cr030116o>.
- Shoemaker DD, Lashkari DA, Morris D, Mittmann M, Davis RW. 1996. Quantitative phenotypic analysis of yeast deletion mutants using a highly parallel molecular bar-coding strategy. *Nat Genet* 14:450–456. <https://doi.org/10.1038/ng1296-450>.
- Giaever G, Shoemaker DD, Jones TW, Liang H, Winzler EA, Astromoff A, Davis RW. 1999. Genomic profiling of drug sensitivities via induced haploinsufficiency. *Nat Genet* 21:278–283. <https://doi.org/10.1038/6791>.
- Azad MA, Wright GD. 2012. Determining the mode of action of bioactive compounds. *Bioorg Med Chem* 20:1929–1939. <https://doi.org/10.1016/j.bmc.2011.10.088>.
- Cardona ST, Selin C, Gislason AS. 2015. Genomic tools to profile antibiotic mode of action. *Crit Rev Microbiol* 41:465–472. <https://doi.org/10.3109/1040841X.2013.866073>.
- Forsyth RA, Haselbeck RJ, Ohlsen KL, Yamamoto RT, Xu H, Trawick JD, Wall D, Wang LBV, Froelich JM, C KG, King P, McCarthy M, Malone C, Misiner B, Robbins D, Tan Z, Zhu ZY, Carr G, Mosca DA, Zamudio C, Foulkes JG, Zyskind JW. 2002. A genome-wide strategy for the identification of essential genes in *Staphylococcus aureus*. *Mol Microbiol* 43:1387–1400. <https://doi.org/10.1046/j.1365-2958.2002.02832.x>.
- Wang J, Soisson SM, Young K, Shoop W, Kodali S, Galgoci A, Painter R, Parthasarathy G, Tang YS, Cummings R, Ha S, Dorso K, Motyl M, Jayasuriya H, Ondeyka J, Herath K, Zhang C, Hernandez L, Allocco J, Basilio A, Tormo JR, Genilloud O, Vicente F, Pelaez F, Colwell L, Lee SH, Michael B, Felcetto T, Gill C, Silver LL, Hermes JD, Bartizal K, Barrett J, Schmatz D, Becker JW, Cully D, Singh SB. 2006. Platensimycin is a selective FabF inhibitor with potent antibiotic properties. *Nature* 441:358–361. <https://doi.org/10.1038/nature04784>.
- Carroll P, Muttucumar DG, Parish T. 2005. Use of a tetracycline-inducible system for conditional expression in *Mycobacterium tuberculosis* and *Mycobacterium smegmatis*. *Appl Environ Microbiol* 71:3077–3084. <https://doi.org/10.1128/AEM.71.6.3077-3084.2005>.
- Judson N, Mekalanos JJ. 2000. TnAraOut, a transposon-based approach to identify and characterize essential bacterial genes. *Nat Biotechnol* 18:740–745. <https://doi.org/10.1038/77305>.
- Wang H, Claveau D, Vaillancourt JP, Roemer T, Meredith TC. 2011. High-frequency transposition for determining antibacterial mode of action. *Nat Chem Biol* 7:720–729. <https://doi.org/10.1038/nchembio.643>.
- Ehrt S, Guo XV, Hickey CM, Ryou M, Monteleone M, Riley LW, Schnappinger D. 2005. Controlling gene expression in mycobacteria with anhydrotetracycline and Tet repressor. *Nucleic Acids Res* 33:e21. <https://doi.org/10.1093/nar/gni013>.
- Larson MH, Gilbert LA, Wang X, Lim WA, Weissman JS, Qi LS. 2013. CRISPR interference (CRISPRi) for sequence-specific control of gene expression. *Nat Protoc* 8:2180–2196. <https://doi.org/10.1038/nprot.2013.132>.
- Peters JM, Colavin A, Shi H, Czarny TL, Larson MH, Wong S, Hawkins JS, Lu CH, Koo BM, Marta E, Shiver AL, Whitehead EH, Weissman JS, Brown ED, Qi LS, Huang KC, Gross CA. 2016. A comprehensive, CRISPR-based functional analysis of essential genes in bacteria. *Cell* 165:1493–1506. <https://doi.org/10.1016/j.cell.2016.05.003>.
- Blomberg A. 2011. Measuring growth rate in high-throughput growth phenotyping. *Curr Opin Biotechnol* 22:94–102. <https://doi.org/10.1016/j.copbio.2010.10.013>.
- Bentley DR, Balasubramanian S, Swerdlow HP, Smith GP, Milton J, Brown CG, Hall KP, Evers DJ, Barnes CL, Bignell HR, Boutell JM, Bryant J, Carter RJ, Keira Cheetham R, Cox AJ, Ellis DJ, Flatbush MR, Gormley NA, Humphray SJ, Irving LJ, Karbelashvili MS, Kirk SM, Li H, Liu X, Maisinger KS, Murray LJ, Obradovic B, Ost T, Parkinson ML, Pratt MR, Rasolonjatovo IM, Reed MT, Rigatti R, Rodighiero C, Ross MT, Sabot A, Sankar SV, Scally A, Schroth GP, Smith ME, Smith VP, Spiridou A, Torrance PE, Tzonev SS, Vermaas EH, Walter K, Wu X, Zhang L, Alam MD, Anastasi C, Aniebo IC, Bailey DM, Bancarz IR, Banerjee S, Barbour SG, Baybayan PA, Benoit VA, Benson KF, Bevis C, Black PJ, Boodhun A, Brennan JS, Bridgman JA, Brown RC, Brown AA, Buermann DH, Bundu AA, Burrows JC, Carter NP, Castillo N, Chiara M, Catenazzi E, Chang S, Neil Cooley R, Crake NR, Dada OO, Diakoumakos KD, Dominguez-Fernandez B, Earnshaw DJ, Egbujor UC, Elmore DW, Etchin SS, Ewan MR, Fedurco M, Fraser LJ, Fuentes Fajardo KV, Scott Furey W, George D, Gietzen KJ, Goddard CP, Golda GS, Granieri PA, Green DE, Gustafson DL, Hansen NF, Harnish K, Haudenschild CD, Heyer NI, Hims MM, Ho JT, Horgan AM, Hoschler K, Hurwitz S, Ivanov DV, Johnson MQ, James T, Huw Jones TA, Kang GD, Kerelska TH, Kersey AD, Khrebtkova I, Kindwall AP, Kingsbury Z, Kokko-Gonzales PI, Kumar A, Laurent MA, Lawley CT, Lee SE, Lee X, Liao AK, Loch JA, Lok M, Luo S, Mammen RM, Martin JW, McCauley PG, McNitt P, Mehta P, Moon KW, Mullens JW, Newington T, Ning Z, Ling Ng B, Novo SM, O'Neill MJ, Osborne MA, Osnowski A, Ostadan O, Paraschos LL, Pickering L, Pike AC, Pike AC, Pinkard CD, Pliskin DP, Podhasky J, Quijano VJ, Raczky C, Rae VH, Rawlings SR, Chiva Rodriguez A, Roe PM, Rogers J, Robert Bacigalupo MC, Romanov N, Romieu A, Roth RK, Rourke NJ, Ruediger ST, Rusman E, Sanches-Kuiper RM, Schenker MR, Seoane JM, Shaw RJ, Shiver MK, Short SW, Sizto NL, Sluis JP, Smith MA, Sohna E, Sohna J, Spence EJ, Stevens K, Sutton N, Szajkowski L, Tregidgo CL, Turcatti G, Vandevondele S, Verhovskiy Y, Virk SM, Wakelin S, Walcott GC, Wang J, Worsley GJ, Yan J, Yau L, Zuerlein M, Rogers J, Mullikin JC, Hurler ME, McCooke NJ, West JS, Oaks FL, Lundberg PL, Klenerman D, Durbin R, Smith AJ. 2008. Accurate whole human genome sequencing using reversible terminator chemistry. *Nature* 456:53–59. <https://doi.org/10.1038/nature07517>.
- Xu HH, Trawick JD, Haselbeck RJ, Forsyth RA, Yamamoto RT, Archer R, Patterson J, Allen M, Froelich JM, Taylor I, Nakaji D, Maile R, Kedar GC, Pilcher M, Brown-Driver V, McCarthy M, Files A, Robbins D, King P, Sillaots S, Malone C, Zamudio CS, Roemer T, Wang L, Youngman PJ, Wall

- D. 2010. *Staphylococcus aureus* TargetArray: comprehensive differential essential gene expression as a mechanistic tool to profile antibacterials. *Antimicrob Agents Chemother* 54:3659–3670. <https://doi.org/10.1128/AAC.00308-10>.
25. Smith AM, Heisler LE, Mellor J, Kaper F, Thompson MJ, Chee M, Roth FP, Giaever G, Nislow C. 2009. Quantitative phenotyping via deep barcode sequencing. *Genome Res* 19:1836–1842. <https://doi.org/10.1101/gr.093955.109>.
  26. Bloodworth RA, Gislason AS, Cardona ST. 2013. *Burkholderia cenocepacia* conditional growth mutant library created by random promoter replacement of essential genes. *Microbiol Open* 2:243–258. <https://doi.org/10.1002/mbo3.71>.
  27. Cardona ST, Mueller C, Valvano MA. 2006. Identification of essential operons in *Burkholderia cenocepacia* with a rhamnose inducible promoter. *Appl Environ Microbiol* 72:2547–2555. <https://doi.org/10.1128/AEM.72.4.2547-2555.2006>.
  28. Lewis RJ, Tsai FT, Wigley DB. 1996. Molecular mechanisms of drug inhibition of DNA gyrase. *Bioessays* 18:661–671. <https://doi.org/10.1002/bies.950180810>.
  29. Varga JJ, Losada L, Zelazny AM, Kim M, McCarrison J, Brinkac L, Sampaio EP, Greenberg DE, Singh I, Heiner C, Ashby M, Nierman WC, Holland SM, Goldberg JB. 2013. Draft genome sequences of *Burkholderia cenocepacia* ET12 lineage strains K56-2 and BC7. *Genome Announc* 1:e00841-13. <https://doi.org/10.1128/genomeA.00841-13>.
  30. Ortega XP, Cardona ST, Brown AR, Loutet SA, Flannagan RS, Campopiano DJ, Govan JR, Valvano MA. 2007. A putative gene cluster for aminoarabinose biosynthesis is essential for *Burkholderia cenocepacia* viability. *J Bacteriol* 189:3639–3644. <https://doi.org/10.1128/JB.00153-07>.
  31. Flannagan RS, Linn T, Valvano MA. 2008. A system for the construction of targeted unmarked gene deletions in the genus *Burkholderia*. *Environ Microbiol* 10:1652–1660. <https://doi.org/10.1111/j.1462-2920.2008.01576.x>.
  32. Mao X, Ma Q, Zhou C, Chen X, Zhang H, Yang J, Mao F, Lai W, Xu Y. 2014. DOOR 2.0: presenting operons and their functions through dynamic and integrated views. *Nucleic Acids Res* 42:D654–D659. <https://doi.org/10.1093/nar/gkt1048>.
  33. Winsor GL, Khaira B, Van Rossum T, Lo R, Whiteside MD, Brinkman FS. 2008. The *Burkholderia* Genome Database: facilitating flexible queries and comparative analyses. *Bioinformatics* 24:2803–2804. <https://doi.org/10.1093/bioinformatics/btn524>.
  34. Lomovskaya O, Warren MS, Lee A, Galazzo J, Fronko R, Lee M, Blais J, Cho D, Chamberland S, Renau T, Leger R, Hecker S, Watkins W, Hoshino K, Ishida H, Lee VJ. 2001. Identification and characterization of inhibitors of multidrug resistance efflux pumps in *Pseudomonas aeruginosa*: novel agents for combination therapy. *Antimicrob Agents Chemother* 45:105–116. <https://doi.org/10.1128/AAC.45.1.105-116.2001>.
  35. Donald RGK, Skwish S, Forsyth RA, Anderson JW, Zhong T, Burns C, Lee S, Meng X, LoCastro L, Jarantow LW, Martin J, Lee SH, Taylor I, Robbins D, Malone C, Wang L, Zamudio CS, Youngman PJ, Phillips JW. 2009. A *Staphylococcus aureus* fitness test platform for mechanism-based profiling of antibacterial compounds. *Chem Biol* 16:826–836. <https://doi.org/10.1016/j.chembiol.2009.07.004>.
  36. Davis BD. 1987. Mechanism of bactericidal action of aminoglycosides. *Microbiol Rev* 51:341–350.
  37. Gellert M, Mizuuchi K, O'Dea MH, Nash HA. 1976. DNA gyrase: an enzyme that introduces superhelical turns into DNA. *Proc Natl Acad Sci U S A* 73:3872–3876. <https://doi.org/10.1073/pnas.73.11.3872>.
  38. Gellert M, O'Dea MH, Itoh T, Tomizawa J. 1976. Novobiocin and coumermycin inhibit DNA supercoiling catalyzed by DNA gyrase. *Proc Natl Acad Sci U S A* 73:4474–4478. <https://doi.org/10.1073/pnas.73.12.4474>.
  39. Aubel-Sadron G, Londos-Gagliardi D. 1984. Daunorubicin and doxorubicin, anthracycline antibiotics, a physicochemical and biological review. *Biochimie* 66:333–352. [https://doi.org/10.1016/0300-9084\(84\)90018-X](https://doi.org/10.1016/0300-9084(84)90018-X).
  40. Buck MA, Cooperman BS. 1990. Single protein omission reconstitution studies of tetracycline binding to the 30S subunit of *Escherichia coli* ribosomes. *Biochemistry* 29:5374–5379. <https://doi.org/10.1021/bi00474a024>.
  41. Khan MA, Mustafa J, Musarrat J. 2003. Mechanism of DNA strand breakage induced by photosensitized tetracycline–Cu(II) complex. *Mutat Res* 525:109–119. [https://doi.org/10.1016/S0027-5107\(03\)00008-3](https://doi.org/10.1016/S0027-5107(03)00008-3).
  42. Khan MA, Musarrat J. 2003. Interactions of tetracycline and its derivatives with DNA in vitro in presence of metal ions. *Int J Biol Macromol* 33:49–56. [https://doi.org/10.1016/S0141-8130\(03\)00066-7](https://doi.org/10.1016/S0141-8130(03)00066-7).
  43. Falagas ME, Kasiakou SK, Saravolatz LD. 2005. Colistin: the revival of polymyxins for the management of multidrug-resistant gram-negative bacterial infections. *Clin Infect Dis* 40:1333–1341. <https://doi.org/10.1086/429323>.
  44. Ferrandiz MJ, Martin-Galiano AJ, Arnanz C, Zimmerman T, de la Campa AG. 2015. Reactive oxygen species contribute to the bactericidal effects of the fluoroquinolone moxifloxacin in *Streptococcus pneumoniae*. *Antimicrob Agents Chemother* 60:409–417. <https://doi.org/10.1128/AAC.02299-15>.
  45. Sampson TR, Liu X, Schroeder MR, Kraft CS, Burd EM, Weiss DS. 2012. Rapid killing of *Acinetobacter baumannii* by polymyxins is mediated by a hydroxyl radical death pathway. *Antimicrob Agents Chemother* 56:5642–5649. <https://doi.org/10.1128/AAC.00756-12>.
  46. Gallagher LA, Shendure J, Manoil C. 2011. Genome-scale identification of resistance functions in *Pseudomonas aeruginosa* using Tn-seq. *mBio* 2:e00315–10. <https://doi.org/10.1128/mBio.00315-10>.
  47. Wetmore KM, Price MN, Waters RJ, Lamson JS, He J, Hoover CA, Blow MJ, Bristow J, Butland G, Arkin AP, Deutschbauer A. 2015. Rapid quantification of mutant fitness in diverse bacteria by sequencing randomly bar-coded transposons. *mBio* 6:e00306–15. <https://doi.org/10.1128/mBio.00306-15>.
  48. Oh J, Fung E, Schlecht U, Davis RW, Giaever G, St Onge RP, Deutschbauer A, Nislow C. 2010. Gene annotation and drug target discovery in *Candida albicans* with a tagged transposon mutant collection. *PLoS Pathog* 6:e1001140. <https://doi.org/10.1371/journal.ppat.1001140>.
  49. Stock AM, Robinson VL, Goudreau PN. 2000. Two-component signal transduction. *Annu Rev Biochem* 69:183–215. <https://doi.org/10.1146/annurev.biochem.69.1.183>.
  50. Stephenson K, Hoch JA. 2002. Virulence- and antibiotic resistance-associated two-component signal transduction systems of Gram-positive pathogenic bacteria as targets for antimicrobial therapy. *Pharmacol Ther* 93:293–305. [https://doi.org/10.1016/S0163-7258\(02\)00198-5](https://doi.org/10.1016/S0163-7258(02)00198-5).
  51. Comenge Y, Quintiliani R, Jr, Li L, Dubost L, Brouard JP, Hugonnet JE, Arthur M. 2003. The CroRS two-component regulatory system is required for intrinsic beta-lactam resistance in *Enterococcus faecalis*. *J Bacteriol* 185:7184–7192. <https://doi.org/10.1128/JB.185.24.7184-7192.2003>.
  52. Muller C, Plesiat P, Jeannot K. 2011. A two-component regulatory system interconnects resistance to polymyxins, aminoglycosides, fluoroquinolones, and  $\beta$ -lactams in *Pseudomonas aeruginosa*. *Antimicrob Agents Chemother* 55:1211–1221. <https://doi.org/10.1128/AAC.01252-10>.
  53. Hirakawa H, Nishino K, Hirata T, Yamaguchi A. 2003. Comprehensive studies of drug resistance mediated by overexpression of response regulators of two-component signal transduction systems in *Escherichia coli*. *J Bacteriol* 185:1851–1856. <https://doi.org/10.1128/JB.185.6.1851-1856.2003>.
  54. Baranova N, Nikaido H. 2002. The *baeSR* two-component regulatory system activates transcription of the *yegMNOB* (*mdtABCD*) transporter gene cluster in *Escherichia coli* and increases its resistance to novobiocin and deoxycholate. *J Bacteriol* 184:4168–4176. <https://doi.org/10.1128/JB.184.15.4168-4176.2002>.
  55. Nishino K, Yamaguchi A. 2002. EvgA of the two-component signal transduction system modulates production of the *yhiUV* multidrug transporter in *Escherichia coli*. *J Bacteriol* 184:2319–2323. <https://doi.org/10.1128/JB.184.8.2319-2323.2002>.
  56. Deng Z, Shan Y, Pan Q, Gao X, Yan A. 2013. Anaerobic expression of the *gadE-mdtEF* multidrug efflux operon is primarily regulated by the two-component system ArcBA through antagonizing the H-NS mediated repression. *Front Microbiol* 4:194. <https://doi.org/10.3389/fmicb.2013.00194>.
  57. Marchand I, Damier-Piolle L, Courvalin P, Lambert T. 2004. Expression of the RND-type efflux pump AdeABC in *Acinetobacter baumannii* is regulated by the AdeRS two-component system. *Antimicrob Agents Chemother* 48:3298–3304. <https://doi.org/10.1128/AAC.48.9.3298-3304.2004>.
  58. White DG, Goldman JD, Demple B, Levy SB. 1997. Role of the *acrAB* locus in organic solvent tolerance mediated by expression of *marA*, *soxS*, or *robA* in *Escherichia coli*. *J Bacteriol* 179:6122–6126.
  59. Gunn JS, Miller SI. 1996. PhoP-PhoQ activates transcription of *pmrAB*, encoding a two-component regulatory system involved in *Salmonella typhimurium* antimicrobial peptide resistance. *J Bacteriol* 178:6857–6864.
  60. Vogt SL, Raivio TL. 2012. Just scratching the surface: an expanding view of the Cpx envelope stress response. *FEMS Microbiol Lett* 326:2–11. <https://doi.org/10.1111/j.1574-6968.2011.02406.x>.
  61. Svensson SL, Davis LM, MacKichan JK, Allan BJ, Pajaniappan M, Thomp-

- son SA, Gaynor EC. 2009. The CprS sensor kinase of the zoonotic pathogen *Campylobacter jejuni* influences biofilm formation and is required for optimal chick colonization. *Mol Microbiol* 71:253–272. <https://doi.org/10.1111/j.1365-2958.2008.06534.x>.
62. Ji Q, Chen PJ, Qin G, Deng X, Hao Z, Wawrzak Z, Yeo WS, Quang JW, Cho H, Luo GZ, Weng X, You Q, Luan CH, Yang X, Bae T, Yu K, Jiang H, He C. 2016. Structure and mechanism of the essential two-component signal-transduction system WalkR in *Staphylococcus aureus*. *Nat Commun* 7:11000. <https://doi.org/10.1038/ncomms11000>.
  63. Delcour AH. 2009. Outer membrane permeability and antibiotic resistance. *Biochim Biophys Acta* 1794:808–816. <https://doi.org/10.1016/j.bbapap.2008.11.005>.
  64. Fraud S, Poole K. 2011. Oxidative stress induction of the MexXY multidrug efflux genes and promotion of aminoglycoside resistance development in *Pseudomonas aeruginosa*. *Antimicrob Agents Chemother* 55:1068–1074. <https://doi.org/10.1128/AAC.01495-10>.
  65. Hwang S, Zhang Q, Ryu S, Jeon B. 2012. Transcriptional regulation of the CmeABC multidrug efflux pump and the KatA catalase by CosR in *Campylobacter jejuni*. *J Bacteriol* 194:6883–6891. <https://doi.org/10.1128/JB.01636-12>.
  66. Fetar H, Gilmour C, Klinoski R, Daigle DM, Dean CR, Poole K. 2011. *mexEF-oprN* multidrug efflux operon of *Pseudomonas aeruginosa*: regulation by the MexT activator in response to nitrosative stress and chloramphenicol. *Antimicrob Agents Chemother* 55:508–514. <https://doi.org/10.1128/AAC.00830-10>.
  67. van der Heijden J, Reynolds LA, Deng W, Mills A, Scholz R, Imami K, Foster LJ, Duong F, Finlay BB. 2016. Salmonella rapidly regulates membrane permeability to survive oxidative stress. *mBio* 7:e01238–16. <https://doi.org/10.1128/mBio.01238-16>.
  68. Taylor BL, Zhulin IB. 1999. PAS domains: internal sensors of oxygen, redox potential, and light. *Microbiol Mol Biol Rev* 63:479–506.
  69. Cardona ST, Valvano MA. 2005. An expression vector containing a rhamnose-inducible promoter provides tightly regulated gene expression in *Burkholderia cenocepacia*. *Plasmid* 54:219–228. <https://doi.org/10.1016/j.plasmid.2005.03.004>.
  70. Pickering BS, Oresnik IJ. 2010. The twin arginine transport system appears to be essential for viability in *Sinorhizobium meliloti*. *J Bacteriol* 192:5173–5180. <https://doi.org/10.1128/JB.00206-10>.
  71. Wong YC, Abd El Ghany M, Naeem R, Lee KW, Tan YG, Pain A, Nathan S. 2016. Candidate essential genes in *Burkholderia cenocepacia* J2315 identified by genome-wide TraDIS. *Front Microbiol* 7:1288. <https://doi.org/10.3389/fmicb.2016.01288>.
  72. Svensson SL, Hyunh S, Parker CT, Gaynor EC. 2015. The *Campylobacter jejuni* CprRS two-component regulatory system regulates aspects of the cell envelope. *Mol Microbiol* 96:189–209. <https://doi.org/10.1111/mmi.12927>.
  73. Martin PK, Li T, Sun D, Biek DP, Schmid MB. 1999. Role in cell permeability of an essential two-component system in *Staphylococcus aureus*. *J Bacteriol* 181:3666–3673.
  74. Shi L, Gunther S, Hubschmann T, Wick LY, Harms H, Muller S. 2007. Limits of propidium iodide as a cell viability indicator for environmental bacteria. *Cytometry A* 71:592–598.
  75. Gotoh Y, Eguchi Y, Watanabe T, Okamoto S, Doi A, Utsumi R. 2010. Two-component signal transduction as potential drug targets in pathogenic bacteria. *Curr Opin Microbiol* 13:232–239. <https://doi.org/10.1016/j.mib.2010.01.008>.
  76. Worthington RJ, Blackledge MS, Melander C. 2013. Small-molecule inhibition of bacterial two-component systems to combat antibiotic resistance and virulence. *Future Med Chem* 5:1265–1284. <https://doi.org/10.4155/fmc.13.58>.
  77. Shen Z, Qu W, Wang W, Lu Y, Wu Y, Li Z, Hang X, Wang X, Zhao D, Zhang C. 2010. MPprimer: a program for reliable multiplex PCR primer design. *BMC Bioinformatics* 11:143. <https://doi.org/10.1186/1471-2105-11-143>.
  78. Schmieder R, Edwards R. 2011. Quality control and preprocessing of metagenomic datasets. *Bioinformatics* 27:863–864. <https://doi.org/10.1093/bioinformatics/btr026>.
  79. Altschul SF, Gish W, Miller W, Myers EW, Lipman DJ. 1990. Basic local alignment search tool. *J Mol Biol* 215:403–410. [https://doi.org/10.1016/S0022-2836\(05\)80360-2](https://doi.org/10.1016/S0022-2836(05)80360-2).
  80. Craig FF, Coote JG, Parton R, Freer JH, Gilmour NJ. 1989. A plasmid which can be transferred between *Escherichia coli* and *Pasteurella haemolytica* by electroporation and conjugation. *J Gen Microbiol* 135:2885–2890.
  81. Rajendran R, Quinn RF, Murray C, McCulloch E, Williams C, Ramage G. 2010. Efflux pumps may play a role in tigecycline resistance in *Burkholderia* species. *Int J Antimicrob Agents* 36:151–154. <https://doi.org/10.1016/j.ijantimicag.2010.03.009>.
  82. Mahenthiralingam E, Coenye T, Chung JW, Speert DP, Govan JR, Taylor P, Vandamme P. 2000. Diagnostically and experimentally useful panel of strains from the *Burkholderia cenocepacia* complex. *J Clin Microbiol* 38:910–913.
  83. Miller VL, Mekalanos JJ. 1988. A novel suicide vector and its use in construction of insertion mutations: osmoregulation of outer membrane proteins and virulence determinants in *Vibrio cholerae* requires *toxR*. *J Bacteriol* 170:2575–2583.
  84. Figurski DH, Helinski DR. 1979. Replication of an origin-containing derivative of plasmid RK2 dependent on a plasmid function provided in trans. *Proc Natl Acad Sci USA* 76:1648–1652.